②

NPS-53-90-006

AD-A224 076

NAVAL POSTGRADUATE SCHOOL
Monterey, California

DTIC
ELECTE
JUL 19 1990
D

SENSITIVITY OF THE ERROR IN
MULTIVARIATE STATISTICAL INTERPOLATION
TO PARAMETER VALUES

by

Richard Franke

Technical Report for Period

October 1987-March 1990

Approved for public release; distribution unlimited

90 07 16 388

NAVAL POSTGRADUATE SCHOOL
MONTEREY CALIFORNIA 93943

Rear Admiral R. W. West, Jr.   Harrison Shull
Superintendent   Provost

Prepared by:

RICHARD FRANKE
Professor of Mathematics

Reviewed by: Released by:

HAROLD M. FREDRICKSEN   G. E. SCHACHER
Chairman   Dean of Faculty and Graduate
Department of Mathematics   Education

REPORT DOCUMENTATION PAGE		Form Approved OMB No 0704-0188

6a NAME OF PERFORMING ORGANIZATION Naval Postgraduate School	6b OFFICE SYMBOL (If applicable) MA	7a. NAME OF MONITORING ORGANIZATION Naval Postgraduate School
6c. ADDRESS (City, State, and ZIP Code) Monterey, CA 93943		7b ADDRESS (City, State, and ZIP Code) Monterey, CA 93943

8a NAME OF FUNDING/SPONSORING ORGANIZATION Naval Postgraduate School	8b OFFICE SYMBOL (If applicable) MA	9 PROCUREMENT INSTRUMENT IDENTIFICATION NUMBER O&MN Direct Funding
8c. ADDRESS (City, State, and ZIP Code) Monterey, CA 93943		10 SOURCE OF FUNDING NUMBERS

PROGRAM ELEMENT NO	PROJECT NO	TASK NO	WORK UNIT ACCESSION NO

11 TITLE (Include Security Classification)

Sensitivity of the error in multivariate statistical interpolation to parameter values (U)

12 PERSONAL AUTHOR(S)
Richard Franke

13a TYPE OF REPORT Technical Report	13b TIME COVERED FROM 10/87 TO 3/90	14 DATE OF REPORT (Year, Month, Day) 9 March 1990	15 PAGE COUNT 62

16 SUPPLEMENTARY NOTATION

17 COSATI CODES			18 SUBJECT TERMS (Continue on reverse if necessary and identify by block number)
FIELD	GROUP	SUB-GROUP	multivariate optimum interpolation, multivariate statistical interpolation, expect error, missing observations, misspecification of parameters

19 ABSTRACT (Continue on reverse if necessary and identify by block number)

The sensitivity of multivariate optimum interpolation to variations in values of it's parameters is investigated, including missing observation values. The influence of misspecification of observation error and parameters in the spatial correlation function are also considered. The calculations are carried out on three different observations patterns: fairly uniform, partly uniform and partly sparse, and sparse. The decay rate of the correlation function is an important parameter to estimate properly and estimates of height and wind errors should be consistent. (KR)

20 DISTRIBUTION/AVAILABILITY OF ABSTRACT ☒ UNCLASSIFIED/UNLIMITED ☐ SAME AS RPT ☐ DTIC USERS	21 ABSTRACT SECURITY CLASSIFICATION UNCLASSIFIED
22a NAME OF RESPONSIBLE INDIVIDUAL Richard Franke	22b TELEPHONE (Include Area Code) 408-646-2758	22c OFFICE SYMBOL MA/FE

1.0 INTRODUCTION

The purpose of this study is to document the sensitivity of multivariate statistical interpolation to the values of statistical parameters, misspecification of these parameters, and to missing observations. It is hoped that this information will enable practitioners to concentrate on the appropriate specification of crucial parameters while avoiding agony over those that have relatively small effect. The results presented here point out some interesting dependencies which I believe have not been previously published. Prior studies upon which this work builds are Franke (1985 and 1988) and especially Franke, et al. (1988). It was also influenced by Seaman (1983). These previous studies, however, involved only univariate objective analysis schemes. While many of the results can be expected to carry over in a similar way, the influence of wind observations on the expected error over various observation sets is useful and interesting. Further, I believe that the graphical presentation of the results used here makes it easy to discern the important parameters.

A brief overview of multivariate statistical interpolation and the method used to calculate expected errors is given in Section 2. The details of the necessary calculations are not given explicitly there, but are available in Appendix 2, which gives a listing of the subroutine used to evaluate the covariance matrices. Section 3 gives a discussion of the various parameters and the values over which they were varied during the study. Section 4 contains an analysis of the results. Because of the plethora of data which was generated it is difficult to comprehend the important details in tabular format, and therefore the information is incorporated into a few graphs which enable one to easily ascertain the sensitivities of the scheme to the various parameters. Tables are included in Appendix 1 for completeness, but it is expected that few readers will find them necessary. Section 5 contains the concluding remarks.

2.0 MULTIVARIATE STATISTICAL INTERPOLATION

Statistical Interpolation (SI) is in use at many of the world's Numerical Weather Prediction (NWP) facilities, including the U.S. Navy's Fleet Numerical Oceanography Center (FNOC). The scheme has its roots in the work of Kolmogorov and Weiner, and was first developed for meteorological applications by Gandin (1965). More recently it has been applied in multivariate form by Schlatter (1975), Schlatter, et al. (1976), Bergman (1979), and Lorenc (1981).

In its perfect form (all parameters known), SI delivers estimates of a field with minimum mean squared error over a certain ensemble of realizations that satisfy normality and stationarity of the underlying stochastic process. For convenience, isotropy is usually assumed, and for meteorological problems a zero mean is assumed (although a nonzero mean can be accounted for in more than one way).

In the multivariate formulation, the dependent data consists of related variables, which in our case we assume to be the errors in the background pressure height and wind fields, H, U, and V, as related through the geostrophic relationship:

$$U = k_1 H_x, \quad V = k_2 H_y \ .$$

Here the values of k_1 and k_2 are dependent on the latitude. The SI equations are applied to the background error, obtained by forming the difference between the background (normally the NWP values, interpolated to the observation locations) and the observed values. The assumption of normality implies the minimum variance (or least mean squared error) predictor is a linear combination of the data values. Then construction of the weights leads to solution of a system of equations whose coefficient matrix is the matrix of spatial covariances and cross-covariances for the variables. Because of the assumed relationship between the variables, the wind error covariances and the cross-covariances are determined when the height error spatial covariance function is known. The exact relationship is given in

2

Franke, et al. (1988), as well as in other references above.

The SI equations have been derived in numerous places (see e.g., Schlatter (1975), Lorenc (1981), Thiébaux (1985), and Thiébaux and Pedder (1987)) and are repeated here only for completeness. Let $O = \{o_j\}_{j=1,\ldots,N}$ represent N measured values, with corresponding independent observation error variance (diagonal) matrix $\Sigma = \{\sigma_j^2\}$, $B = \{b_j\}$ the corresponding vector of background values, and $C = \{c_{i,j}\}_{i,j=1,\ldots,N}$ the spatial covariance matrix for the background errors. Then, letting $C_0 = \{c_{0j}\}_{j=1,\ldots,N}$ denote the vector of covariances between the error in the variable at the location P_0 at which it is to be analyzed and the background errors, the following equation holds for the analyzed value, a_0:

$$a_0 = b_0 + C_0^T(C+\Sigma)^{-1}(O - B) \quad .$$

If the statistical parameters are known precisely (whereupon SI becomes Optimum Interpolation, or OI), then the expected error variance for the estimated variable at P_0 is given in the usual least squares form,

$$\sigma_0^2 = \sigma_b^2 - C_0^T(C+\Sigma)^{-1}C_0 \quad ,$$

where σ_b^2 is the variance of the background error. Considering the case where the statistical parameters are not known exactly, the analyzed value becomes

$$a_0 = b_0 + \tilde{C}_0^T(\tilde{C}+\tilde{\Sigma})^{-1}(O - B) \quad ,$$

where the tilde overbar signifies assumed inexact values. Notice that the equation is exactly the same except that assumed values replace the exact values for covariances. The expected mean squared error is

$$\sigma_0^2 = \sigma_b^2 - 2C_0^T(\tilde{C}+\tilde{\Sigma})^{-1}\tilde{C}_0 + \tilde{C}_0^T(\tilde{C}+\tilde{\Sigma})^{-1}(C+\Sigma)(\tilde{C}+\tilde{\Sigma})^{-1}\tilde{C}_0 \quad .$$

These equations are given in Seaman (1983), where the vector $\tilde{W}_0 = (\tilde{C} + \tilde{\Sigma})^{-1} \tilde{C}_0$ is interpreted in the usual statistical fashion, as the weight vector for the observed minus background values. This also simplifies the writing of the error expression and indicates a computationally efficient algorithm.

The expected error will be computed at a number of locations, in our case on a 7x11 grid of points. The matrix $(\tilde{C} + \tilde{\Sigma})$ is symmetric and positive definite, so the computation of $\tilde{W}_0$ is accomplished by performing a one time Cholesky decomposition of $(\tilde{C} + \tilde{\Sigma})$ into LL^T, followed by forward and backward substitutions to find $\tilde{W}_0$ as the solution of $LL^T W_0 = \tilde{C}_0$. This is an important concept since the number of equations is the number of observations (up to 108 here), and P_0 varies over 77 locations in our case. In actual practice P_0 would vary over several locations for the same observation set when a block analysis scheme is used.

3.0 SETTING FOR THE STUDY

An empirical study such as this one requires a number of compromises concerning the range of parameters permitted. In previous studies (Franke, 1985, and Franke, et al., 1988) a set of three grids and corresponding observation locations based approximately on the radiosonde network over the United States and the Atlantic Ocean were used. The study here is also at a single level. One difference from my previous studies, which has a rather minor influence, is that distances are measured in meters (approximately; I did not use the exact geodesic distance) rather than degrees. The formula used for the distance (also used by Schlatter (1975)) between two points (θ = longitude, φ = latitude) is

$$d_{ij}^2 = r^2 [(\varphi_j - \varphi_i)^2 + (\theta_j - \theta_i)^2 \cos^2(\frac{\varphi_j - \varphi_i}{2})] \ .$$

While computed distances are (relatively) quite different in the upper latitudes, the overall influence on the expected mean squared errors is rather small over the regions we consider.

4

Figures 1-3 show the 2.5° grids and observation locations used in this study. The +'s indicate the grid points, while the small squares and circles represent the observation locations. The shaded circle represents the "missing observation" for tests of sensitivity of the analyzed values to one missing observation (both missing wind only and missing height and wind). The open circles represent additional missing observation locations for tests of sensitivity to many (one-half) missing observations. Each grid is a 7x11 grid of points, taken to be the interior grid points of a 9x13 grid containing the observation locations. The Middle United States (MUS) grid has 36 observations, the East Coast (EC) grid has 25 observation locations, while Middle Atlantic (MA) grid has only 3 observations.

The assumed correlation function for the height errors is the specialized second order autoregressive function (SOAR) that seems to be quite stable with respect to variations in the parameters while embodying enough parameters to fit historical data (Franke, et al., 1988). As noted by Thiébaux, et al. (1986), Balgovind, et al. (1983), the SOAR seems to have an affinity for meteorological data. The form we used is

$$C(s) = (1-A)(1+as)e^{-as} + A,$$

where s denotes the distance, and a and A are parameters which in practice are determined by a fitting process. In the previous section $c_{ij}=C(d_{ij})\sigma_b^2$, where d_{ij} is the distance between the ith and j^{th} observation points. The study conducted here made use of five different sets of parameter values, as shown in Table 1, and also depicted in Figure 4. The "nominal" correlation function is considered to be #4, which approximates the Bessel function curve of Lonnberg (1982) closely, and also corresponds closely to the decay rate used by Lorenc and Hammon (1988). Varying from one correlation function to the next makes it possible to determine whether the additive constant or the decay rate constant is the more critical.

5

Cor#	A	a	#m to #m+1
1	0.0	5.000×10^{-6}	
			a decreases
2	0.0	3.082×10^{-6}	
			A increases
3	0.15	3.082×10^{-6}	
			A increases
4	0.2722	3.082×10^{-6}	
			a decreases
5	0.2722	2.188×10^{-6}	

Table 1: Correlation Functions

The nominal value for the standard deviation of the background height error is 30 m. The correlation function then determines the variance of the wind field errors, and the standard deviations for wind errors are given in Table 2. Because the values of k_1 and k_2 depend on the latitude, the rms errors over a given grid depend on the grid. All expected wind errors were calculated relative to their value at a given point, and the rms values of these are given in the tables and the figures, different than computing the expected rms values over the grid and then comparing this with the rms background error over the grid.

The nominal values assumed for the observation errors were 10 m for heights and 1.0 m/sec for wind components. For OI these values were varied over the values 0, 5, 10, 20, and ∞ m for heights, and 0, 0.5, 1.0, 2.0, and ∞ m/sec for the winds. The expected rms error was not computed for all combinations of these values; the ∞ values imply no measurement of that variable and computations were only performed with the nominal value of the other measurement error, for example. These calculations were performed with OI to show the effect of no observations of a particular variable. With no wind observations, the process collapses to the usual univariate OI scheme.

In order to assess the effect of missing observations, four "missing observation" computations were performed. For one observation point in each grid it was assumed that the wind

6

observations were not available; then it was assumed that the height observation at the same location was not available. For about one-half of the observation points it was assumed that the wind observations were not available; then it was assumed that the corresponding height observations were not available.

The computations of expected rms errors for the statistical schemes did not cover such a wide range of assumed observation error values. Variations of the assumed observation errors and spatial correlation function number were only carried out to the adjacent value (assumed observation error changing by a factor of .5 or 2, and correlation function number only to the adjacent number).

Cor#	grid 1&2	grid 3
1	16.05	14.52
2	9.89	8.95
3	9.12	8.25
4	8.44	7.64
5	5.99	5.42

Table 2: Background wind errors, m/sec

4.0 ANALYSIS OF THE RESULTS

The easy detection of the sensitivity to parameters on which a process depends is sometimes clouded by the mass of information available. In the following, I believe the plotting scheme adopted enables readers to easily detect critical parameters.

In this study there are four important parameters that are varied for each of the three grids: The height observation accuracy, the wind observation accuracy, the additive constant A in the correlation function, and the decay rate a (the reciprocal can be thought of as some measure of "correlation distance") in the correlation function. In this study the correlation function

7

parametᴖs have not been varied except one at a time, in the manner noted in the previous section.

We first consider the sensitivity of OI to the accuracy of the observations. The results for the error in the analyzed height field for 13 different combinations of observation accuracies and 5 correlation functions are shown in Figures 5-7 for the MUS, EC, and MA grids, respectively. Note that only the integer abscissa values have meaning, and the points are connected only to enable one to more easily see the effects of changing parameter values. As one moves to the right on the scale, the trend is toward less observation accuracy, with wind observation accuracies first decreasing, while the height observation accuracy more slowly decreases. From the plots, it is seen that significant increases in OI height analysis errors occur at abscissae 2, 5, 9, and 13, while between there is generally some increase, but much smaller in magnitude. Table 3 lists the values of the observation accuracies, and it is seen that for 2, 5, 10, and 13 there are jumps in the observation accuracy for heights. The jump in expected error at abscissa 9 is due to the complete loss wind observations, and if this abscissa is omitted, then the jump would be due to the height accuracy change at abscissa 10. From this graph it is apparent that the accuracy of height observations are of premier importance in the height analysis, while the accuracy of the wind observations are less important in the nominal range considered here, **except** that not having wind observations at all also results in a significant increase in OI error.

Significant increases in error of the analyzed height field are seen to occur with decreasing correlation distance (increasing value of a) and decreasing constant A, for all three grid and observation point sets. Of course, the effects of observation accuracy are considerably smaller for the sparse MA grid. For all three grids it is apparent that OI errors are more sensitive to changes in the correlation distance (parameter a) than in the additive constant A.

8

abscissa	h error	w error
1	0	1.0
2	5	0.5
3	5	1.0
4	5	2.0
5	10	0.0
6	10	0.5
7	10	1.0
8	10	2.0
9	10	∞
10	20	0.5
11	20	1.0
12	20	2.0
13	∞	1.0

Table 3: Abscissa key for Figures 5-16

The corresponding plots for the errors in the analyzed wind fields are shown in Figures 8-10. The errors shown are the rms of the two winds, the values generally being quite close together, as can be seen by referring to Tables 1.g.m in the Appendix 2. The errors in the analyzed wind fields generally follow the same trend as the errors in the analyzed height fields, except that the wind errors are more sensitive to the wind observation errors, this being especially prominent when there are no wind observations (at abscissa 9). One interesting thing to notice is that the curves for correlation functions 2-4 are very close together, indicating an even greater dependence on the decay rate parameter, a, than the analyzed height errors exhibited.

In order to assess the importance of a single observation and the effects of many missing observations, some OI analysis errors were computed based on missing observed values. The missing observations are shown in Figures 1-3 for the three grids. The expected OI height analysis errors are shown in Figures 11-13 for the three grids, and the expected OI wind analysis errors in Figures 14-16. I will discuss Figure 11 in some detail, and a similar analysis follows for the other figures.

The figure is slightly busy. The open circles and open

squares denote the values for correlation functions #4 and #1, respectively, the same values as given in Figure 5. The same symbol with the + denotes the analyzed values under the same assumptions but with observed values missing (appearing twice; once with observation of winds missing at the location noted previously, the second with observations of both winds and height missing). It can be noted that the missing wind observation is nearly undetectable while there is only a slight degradation with the height observation also missing. This is, however, more prominent in the case of smaller correlation in the upper graph for correlation function #1. The shaded symbols denote the values obtained when one-half (18) of the observations are missing (again, twice, once for missing winds, and once for missing heights and winds). At abscissa 9 the symbol overlays the others for which there are no wind observations and height observations at all locations. The nominal case (abscissa 7) shows about a 15 percent increase in the analysis errors when 18 wind observations are missing, and about a 50 percent increase in the analysis errors for each correlation function when the entire observation is missing at 18 points. In this case, a 15 percent increase in the analysis errors corresponds to about a 6 percent decrease in "skill", where "skill" is taken as (1 - expected analysis error relative to background error), and the 50 percent increase in error to about a 20 percent decrease in skill. The general pattern of error for the various parameter values is generally the same as for that obtained for the entire observation set, the primary difference being for abscissa 9 where the wind observations are all missing.

The OI analyzed height error for the EC grid (Figure 12) follows much the same pattern, except that the increase due to one missing observation is somewhat more significant, the total number of observations being 25 instead of 36 as in the MUS grid. Again, with one-half the observations missing, the error is increased by about 50 percent, and the drop in skill about 25 percent.

The MA grid results in Figure 13 differ since one missing

10

observation is nearly one-half of the total of three. Thus there are no shaded symbols in that figure, and a completely missing observation results in an increase of height analysis error of a few percent, but this again being about a 20 percent drop in skill.

The plots for the wind analysis errors are given in Figures 14-16. Note that some of symbols for separate correlation functions are overlaid in Figures 14 and 15. Of course, the wind analysis is sensitive to the loss of one or more observations, with the increase in wind analysis errors in Figure 14 for the MUS grid showing an increase of about 6-8 percent with 18 missing wind observations, and about 12-15 percent when the entire observation is missing at 18 points. The decrease in skill here corresponds to about 20 percent and 40 percent, respectively. On a relative basis the analysis errors are significantly larger for winds, with smaller relative increases in the error when observations are missing, however, in terms of skill level, the winds are more dependent on the observations. Again, the general character of the errors follows the same pattern, with the exception of abscissa 9, corresponding to no wind observations.

The plots for the wind analysis errors for the EC grid in Figure 15 and the MA grid in Figure 16 reveal no surprises. The general pattern of Figure 15 is similar to Figure 14, while Figure 16 reveals that a very small skill is involved in this case, so missing observations have little affect.

Unfortunately, none of the parameters varied above are really at the disposal of the practitioner. Still, the above information is a useful aid to understanding the OI (and SI) process and how achievable accuracy is affected by the parameters in the process.

The more important practical information is that given in Figures 17-22. Once again, the analysis errors are plotted versus a single abscissa which corresponds to various combinations of assumed parameter values. The nominal background rms error is 30 m for the height, as noted in the previous section, with the background wind errors depending on the

correlation function. Nominal height observation accuracy is 10
m, and nominal wind observation accuracy is 1 m/sec. For a given
spatial correlation function number, the assumed observation
accuracies and spatial correlation function are varied.
Observation accuracies vary by a factor of .5 or 2 from the
nominal, while correlation function number varies by at most one.

Consider Figure 17. The three "curves" for the MUS grid and
spatial correlation functions 2, 3, and 4 will be discussed. As
in previous figures, only the integer abscissa values have
meaning, and the points are connected only to enable one to more
easily see the effects of changing parameter values. It is
immediately apparent that the parameters to which the SI scheme
are most sensitive are embodied in abscissae 9, 12, 13, and to a
lesser extent, 2, 4, and 5. Table 4 shows the relationship
between the abscissae and the parameter variations, and we see
that each of these abscissae except 9 are for assumed height
observation errors that are twice the nominal value, and
abscissae 9, 12, and 13 are for a misspecified correlation
function (greater correlation). Abscissa -8, -9, -10, -11, -12,
and -13 also show relatively larger SI errors, and each of these
abscissa are for low assumed correlation as well as improper
assumed height observation error. It appears that it is better
to underestimate height observation errors than to overestimate
them, although there is a peak (but smaller) at abscissa -2,
where the height observation error is underestimated.

Note that the graphs for correlation functions 3 and 4 are
quite similar, while that for correlation function 2 differs
somewhat for negative abscissae. Table 1 shows that the assumed
correlation function (that is function 1) for large negative
abscissae for correlation function 2 has a different decay rate,
while for correlation functions 3 and 4, the decay rate is the
same as that of 2 and 3. The relatively larger effect of the
improper decay rate for the assumed correlation function is also

12

abscissa	h error	w error	cor f. #
		nominal values	
	10	1	m
		assumed values	
-13	5	0.5	m-1
-12	5	2	m-1
-11	20	0.5	m-1
-10	20	2	m-1
-9	5	1	m-1
-8	20	1	m-1
-7	10	0.5	m-1
-6	10	2	m-1
-5	5	0.5	m
-4	5	2	m
-3	10	1	m-1
-2	5	1	m
-1	10	0.5	m
0	10	1	m
1	10	2	m
2	20	1	m
3	10	1	m+1
4	20	2	m
5	20	0.5	m
6	10	2	m+1
7	10	0.5	m+1
8	20	1	m+1
9	5	1	m+1
10	5	0.5	m+1
11	5	2	m+1
12	20	0.5	m+1
13	20	2	m+1

Table 4:   Abscissa key for Figures 17-22

apparent in the SI error for correlation function 4 at abscissae
9, 12, and 13, as noted above. Thus, the decay rate for the
correlation function seems to be more important than the additive
constant.

For the EC grid, the results shown in Figure 18 indicate
that the character of the three graphs is much the same. The
outstanding difference is the significantly larger SI errors
occurring for correlation function #2 when the assumed
correlation function is #1 (abscissae -3 and -6 to -13). Again,
the graph for correlation function #4 shows larger SI errors for
assumed correlation function #5 (larger abscissae). Both of

these cases correspond to misspecified decay rates. Looking higher to the MA grid, we see same effects: cases where the decay rate for the correlation function is misspecified yield larger increases in the SI height error than when the additive constant is misspecified.

The results for the MA grid shown in Figure 19 imply that the most crucial parameter to have correct in such sparse regions is the decay rate for the correlation function, unfortunately the most difficult to estimate in such cases. Further, it appears it is probably best to underestimate the decay rate in sparse (or semi-sparse regions, such as EC) regions. In data dense regions the height errors are generally less sensitive to misspecification of the correlation function (with the exception of this being in combination with overestimates of the height observation error).

The corresponding plots for SI wind errors are in Figures 20-22. Here the behavior of the errors seems to be less structured, with the smallest error often occurring for the correlation function corresponding to the least spatial correlation (SI height errors are generally a decreasing function of correlation function #). The behavior of the SI wind errors are also sensitive to the misspecification of the decay rate for the correlation function, as can be noted by the correlation function #2 values for large negative abscissae and for correlation function #4 for large positive abscissae. With that exception, the general behavior of the SI wind errors is much the same as for the SI height errors, with the primary dependence again being on the correct specification of the assumed height error.

One additional bit of information can be squeezed from the data generated by this study. This concerns the relationship between the expected error based on the OI calculations versus the actual expected error. Of course, since parameters are estimated, only the expected error for OI can be calculated when expected errors are needed (e.g., see Goerss (1989)). We give three examples to show how this proceeds, and to show the

14

variation in the values. While the information can also be obtained by looking at the appropriate figures, the information is more precisely and as easily obtained from the tables in Appendix 1.

(1) Let us suppose that the assumed values of the observation errors are the twice the nominal ones and that the assumed spatial correlation function is #4. Height and wind observation errors equal 20 m and 2 m/sec, respectively. For the MUS grid the expected error for the heights (from Table 1.1.4, or Figure 5, abscissa 12 on Cor Ftn 4) is 0.3462. If the actual values for the observation errors are 10 m for heights and 1 m for winds, with spatial correlation function #3, then the actual expected error for the MUS grid is (from Table 6.1.3-4, or Figure 17, abscissa 13 on Cor Ftn 3) is 0.3092, significantly smaller than the OI calculation would indicate.

(2) Now suppose the assumed values of the observation errors are one-half the nominal values and that the assumed correlation function is #3. Height and wind observation errors equal 5 m and 0.5 m/sec, respectively. For the MUS grid the expected error for the heights (from Table 1.1.3, or Figure 5, abscissa 2 on Cor Ftn 3) is 0.2291. Again if the correct values are the nominal values of 10 m and 1 m/sec for the height and wind observation errors, and the actual spatial correlation function is #4, then (from Table 6.1.4-3, or Figure 17, abscissa -13 on Cor Ftn 4) the correct expected error is 0.2819. In this case the expected errors are significantly larger than the OI calculation indicates.

(3) In this case, suppose the spatial correlation function is correct, #4, and the assumed values of the observation errors are 5 m and 2 m/sec for heights and winds, respectively. Then the for the EC grid the expected height error (Table 1.2.4, or Figure 6, abscissa 4 on Cor Ftn 4) is 0.3486. If the actual observation errors are 10 m and 1 m/sec for heights and winds, respectively, then the actual expected error (Table 6.2.4-4, or Figure 18, abscissa -4 on Cor Ftn 4) is 0.3870; again the OI expected error is smaller.

As a general rule, expected error as calculated by OI will be optimistic when the observation errors are underestimated or when the spatial correlation is overestimated. The latter usually has a greater influence. On the other hand, when

15

observation errors are overestimated or when the spatial correlation is underestimated, the expected error estimates computed by OI will be pessimistic. Any expected error estimates from operational OI sources should be treated with some caution, the examples above merely serving as an indication of the difficulties and not as a guide to the magnitude of the difference between the computed and actual values that may occur in practice.

5.0 CONCLUDING REMARKS

The results of this study demonstrate that SI analyzed height errors are more sensitive to the decay rate for the spatial correlation function than for the additive constant. While this study concentrated on the SOAR correlation function, similar results can be expected for other correlation functions which are controlled by parameters governing similar properties. The wind errors are even more sensitive to proper values for the decay rate, unsurprising since the wind correction is related to the derivative of the spatial correlation function for the heights.

Another interesting observation is that it is better to "make the same mistake" relative to the observation error for the heights and winds. For example, if observed height error is specified as too large, smaller analysis errors occur when the observed wind errors are also specified as too large, rather than correct or too small. As a general rule, erring on the side of underestimating the observation error seems to result in smaller analysis errors than erring on the side of overestimation of the observation error.

The effect of one missing wind observation is vanishingly small. This is true even when one observation constitutes a significant portion of the total amount of data, as in the MA grid case. However, two things come into play in this case to make the missing data still rather insignificant: (1) the missing data is close to another observation, and (2) the skill in this case is rather low anyway. Missing much data (about

16

one-half) shows significant decreases in skill, about 20-25 percent for heights and up to 40 percent for the winds.

The relationship between the expected error that can be computed using SI and the actual values of the expected error were explored briefly. Practitioners need to be cognizant of the fact that these two values may be significantly different from each other.

REFERENCES

R. Balgovind, A. Dalcher, M. Ghil, and E. Kalnay (1983), A stochastic-dynamic model for the spectral structure of forecast error statistics, **Mon. Wea. Rev.** 111, 701-722.

K. H. Bergman (1979), Multivariate analysis of temperatures and winds using optimum interpolation, **Mon. Wea. Rev.** 107,1423-1444.

R. Franke (1985), Sources of error in objective analysis, **Mon. Wea. Rev.** 113, 260-270.

R. Franke (1988), Statistical interpolation by iteration, **Mon. Wea. Rev.** 116,961-963.

R. Franke, E. Barker, and J. Goerss (1988), The use of observed data for the initial-value problem in numerical weather prediction, **Comput. Math. Applic.** 16,169-184.

L. S. Gandin (1965), **Objective analysis of meteorological fields** (1963), translated from Russian by the Israel Program for Scientific Translations, NTIS TT65-50007.

J. Goerss (1989), Analysis uncertainties determination: Navy Operational Global Atmospheric Prediction System (NOGAPS), TR# 89-09, Naval Environmental Prediction Research Facility, Monterey, CA 93943.

P. Lonnberg (1982), Structure functions and their implications for higher resolution analysis, in **Proceedings of a Workshop on Current Problems in Data Assimilation**, ECMWF, pp. 142-178.

A. C. Lorenc (1981), A global three dimensional multivariate statistical interpolation scheme, **Mon. Wea. Rev.** 109, 701-721.

A. C. Lorenc and O. Hammon (1988), Objective quality control of observations using Bayesian methods. Theory, and a practical implementation, **Q. J. R. Meteorol. Soc.** 114, 515-543.

T. W. Schlatter (1975), Some experiments with a multivariate statistical objective analysis scheme, **Mon. Wea. Rev.** 103, 246-257.

T. W. Schlatter, G. W. Branstator, and L. G. Thiel (1976), Testing a global multivariate statistical objective analysis scheme with observed data, **Mon. Wea. Rev. 104**, 765-783.

R. S. Seaman (1983), Objective analysis accuracies of statistical interpolation and successive correction schemes, **Aust. Met. Mag. 31**, 225-240.

H. J. Thiébaux, (1985), On approximations to geopotential and wind-field correlation structures, **Tellus 37A**, 126-131.

H. J. Thiébaux, H. L. Mitchell, and D. W. Shantz (1986), Horizontal structure of hemispheric forecast error correlations for geopotential and temperature, **Mon. Wea. Rev. 114**, 1048-1066.

H. J. Thiébaux and M. A. Pedder (1987), **Spatial Objective Analysis**, Academic Press, London.
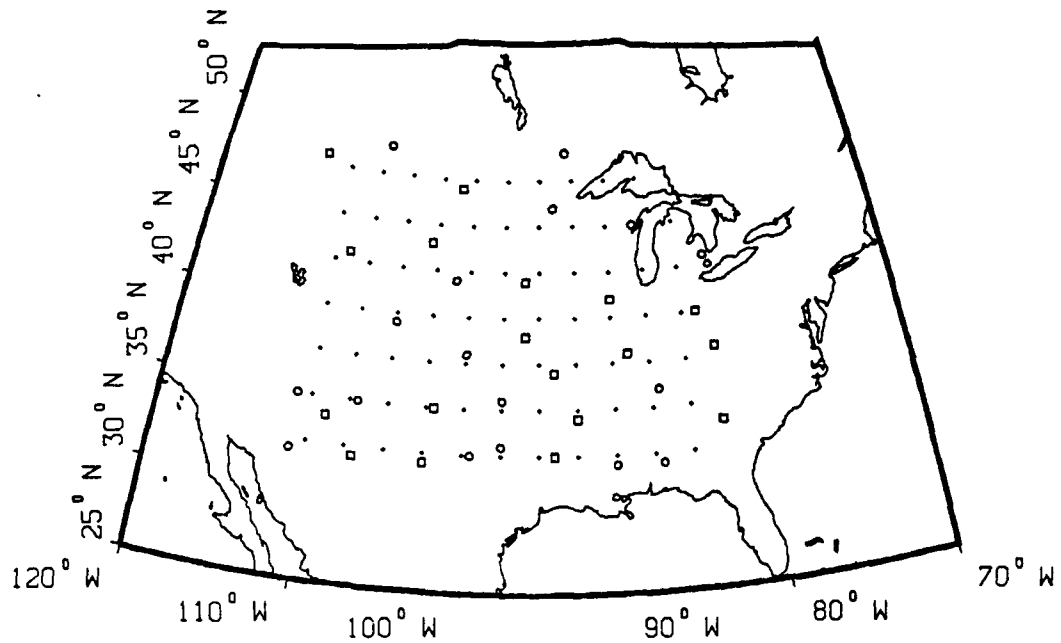
Figure 1: The Middle US (MUS) grid and observation locations. The +'s show the 2.5° grid. The open squares and circles and the shaded circle show observation locations. The shaded circle is a "missing observation" in one test run, and all circles are "missing observations" in another.
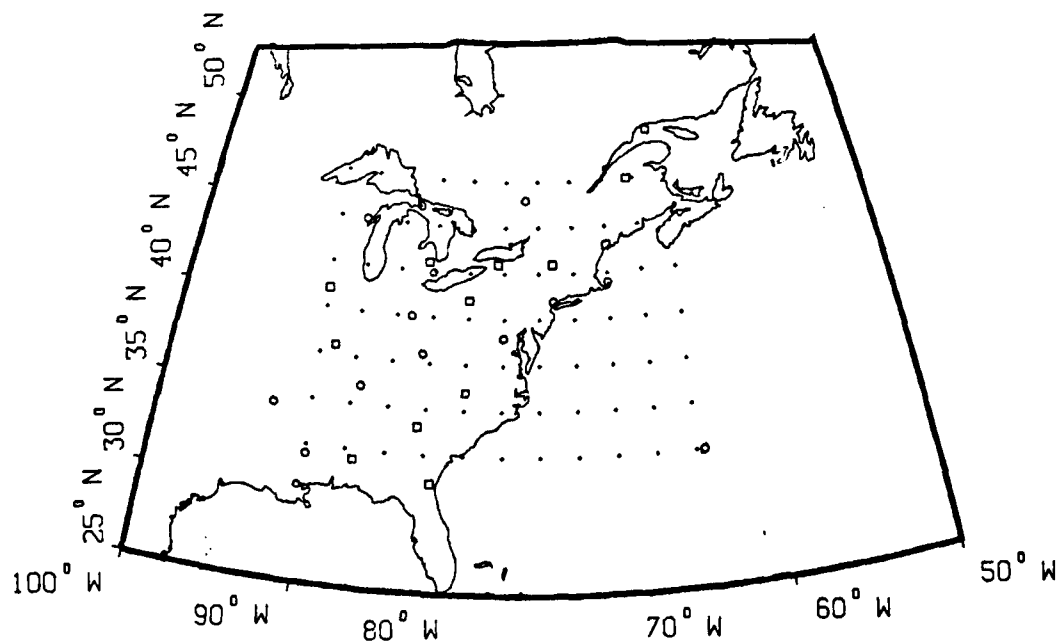
Figure 2: The East Coast (EC) grid and observation locations. Symbols as in Figure 1.

19
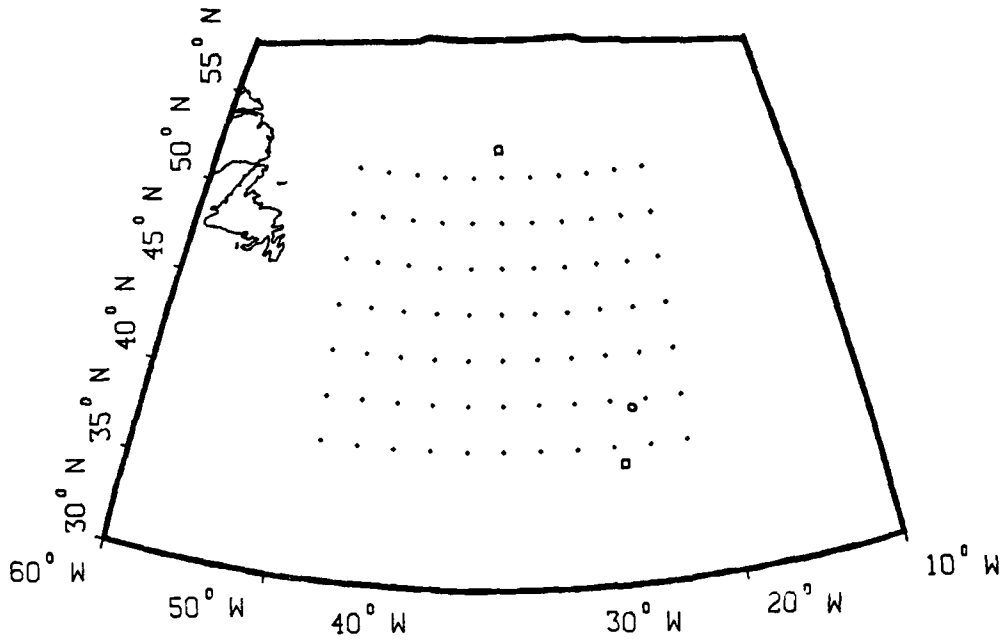
Figure 3: The Middle Atlantic (MA) grid and observation locations. Symbols as in Figure 1, except there is only a single "missing observation".

SPATIAL CORRELATION
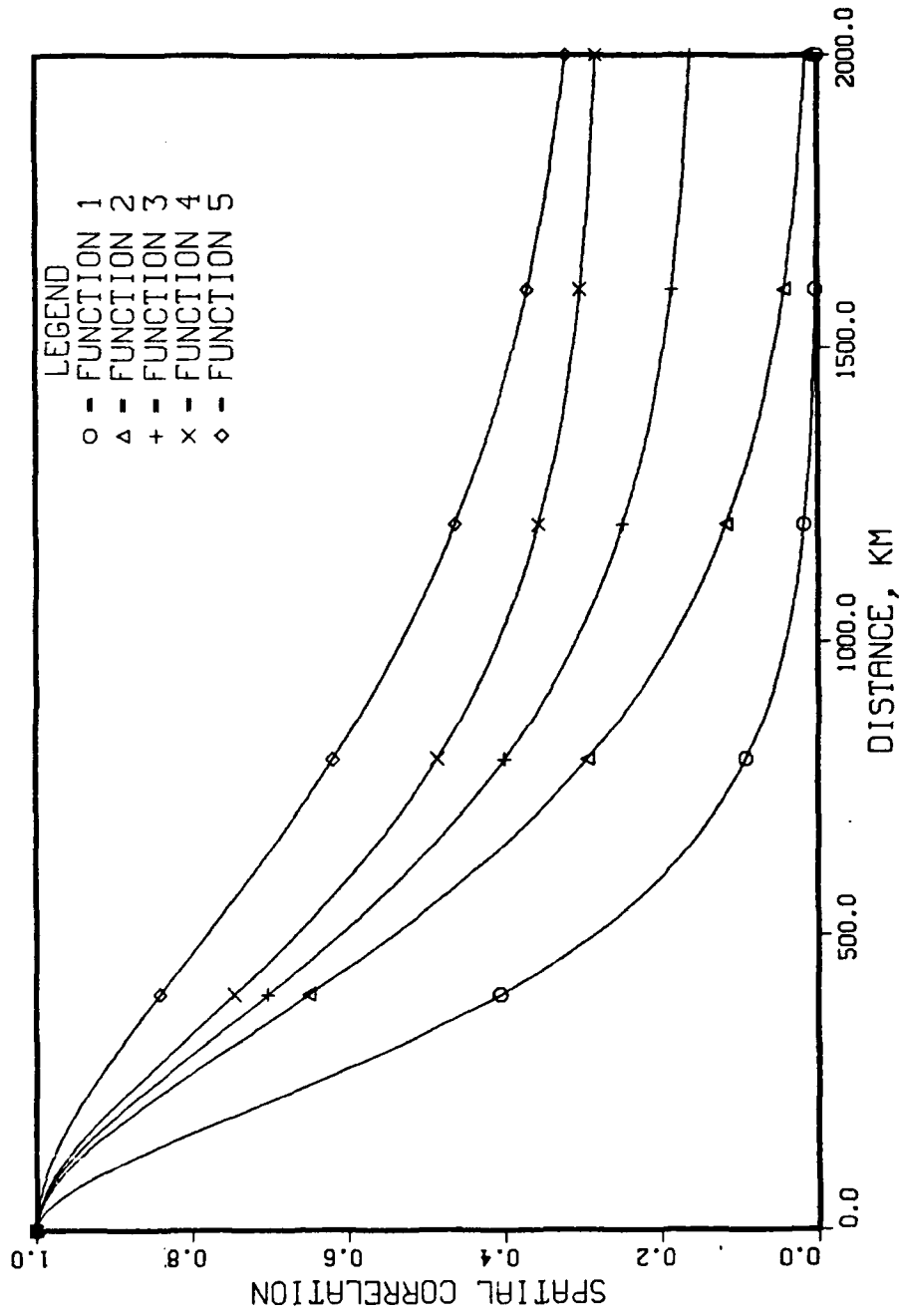
Figure 4: Spatial correlation functions.
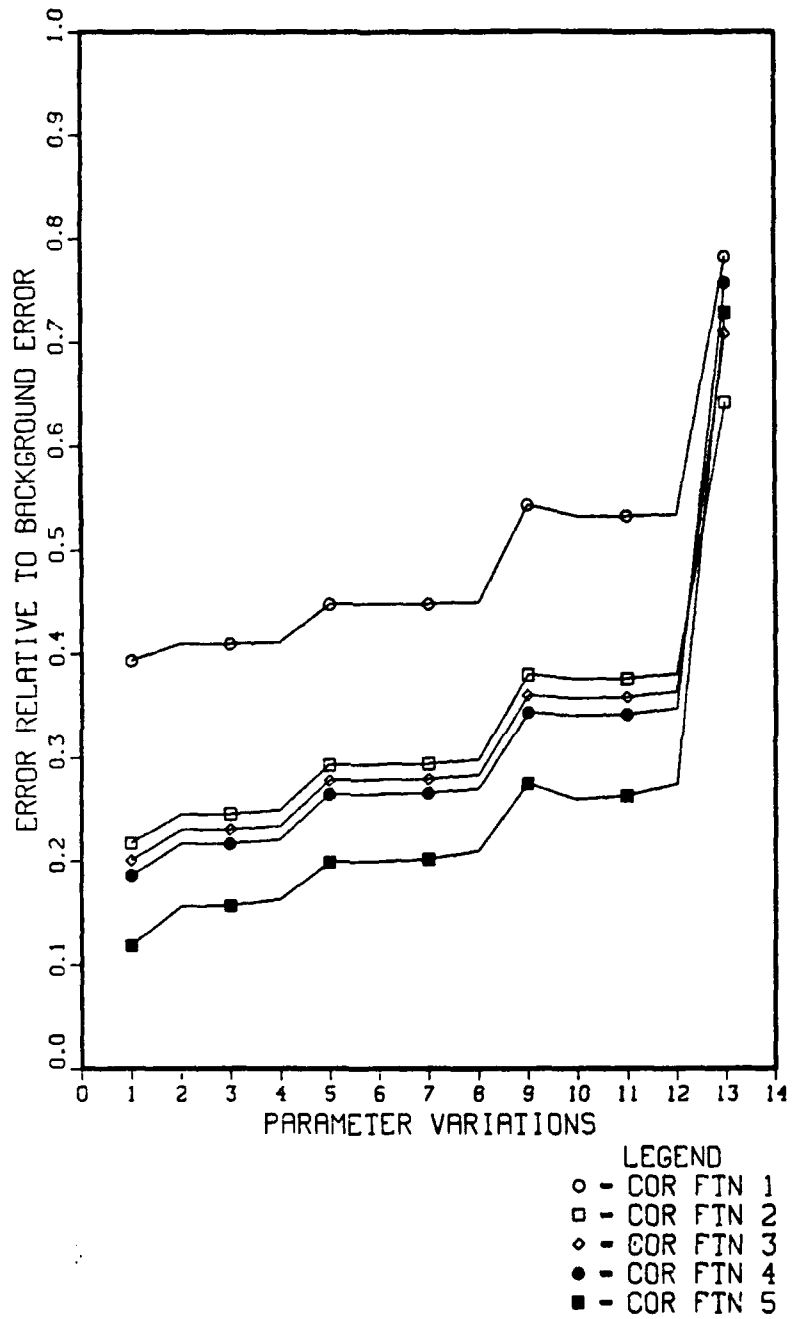
Figure 5: Expected error in OI height analysis under various observation error and spatial correlation function conditions for the MUS grid and observation set.

OI HEIGHT ERRORS, EC GRID
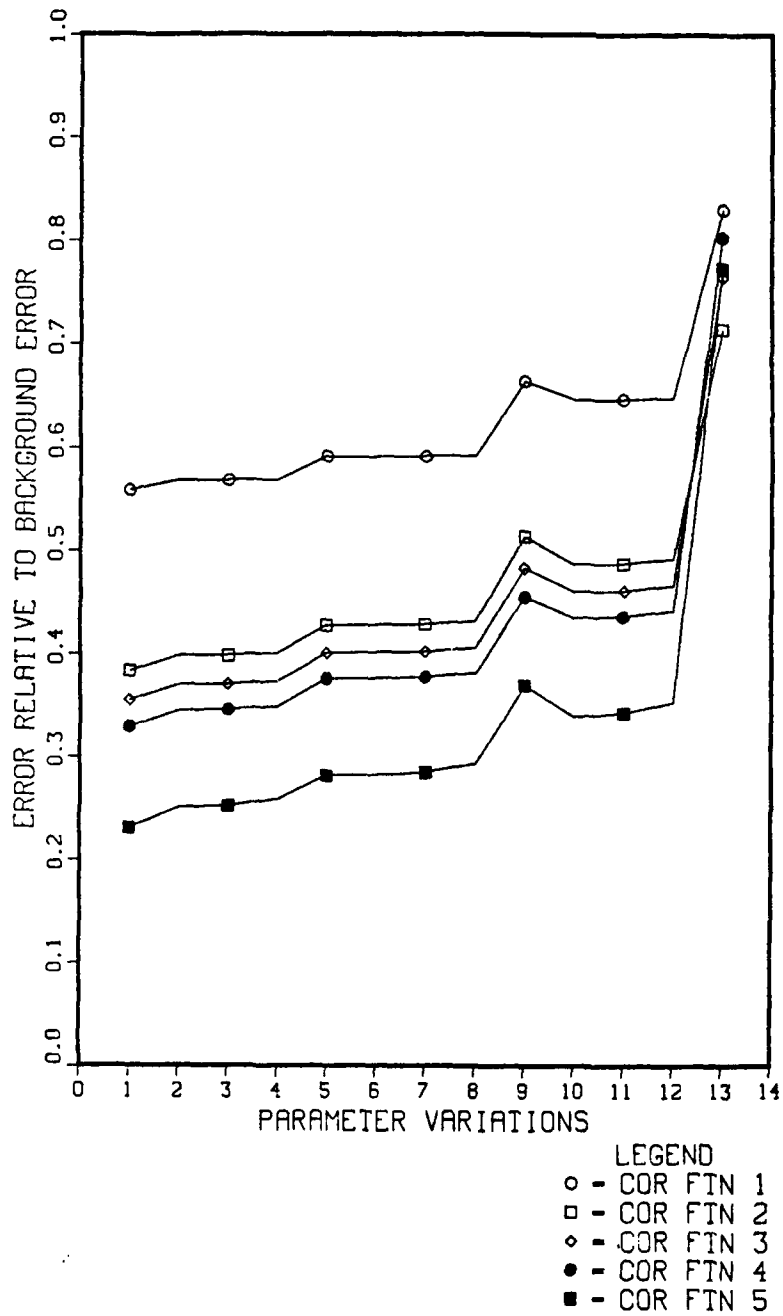
Figure 6: As in Figure 5, for the EC grid and observation set.

OI HEIGHT ERRORS, MA GRID

LEGEND
o — COR FTN 1
□ — COR FTN 2
◇ — COR FTN 3
● — COR FTN 4
■ — COR FTN 5
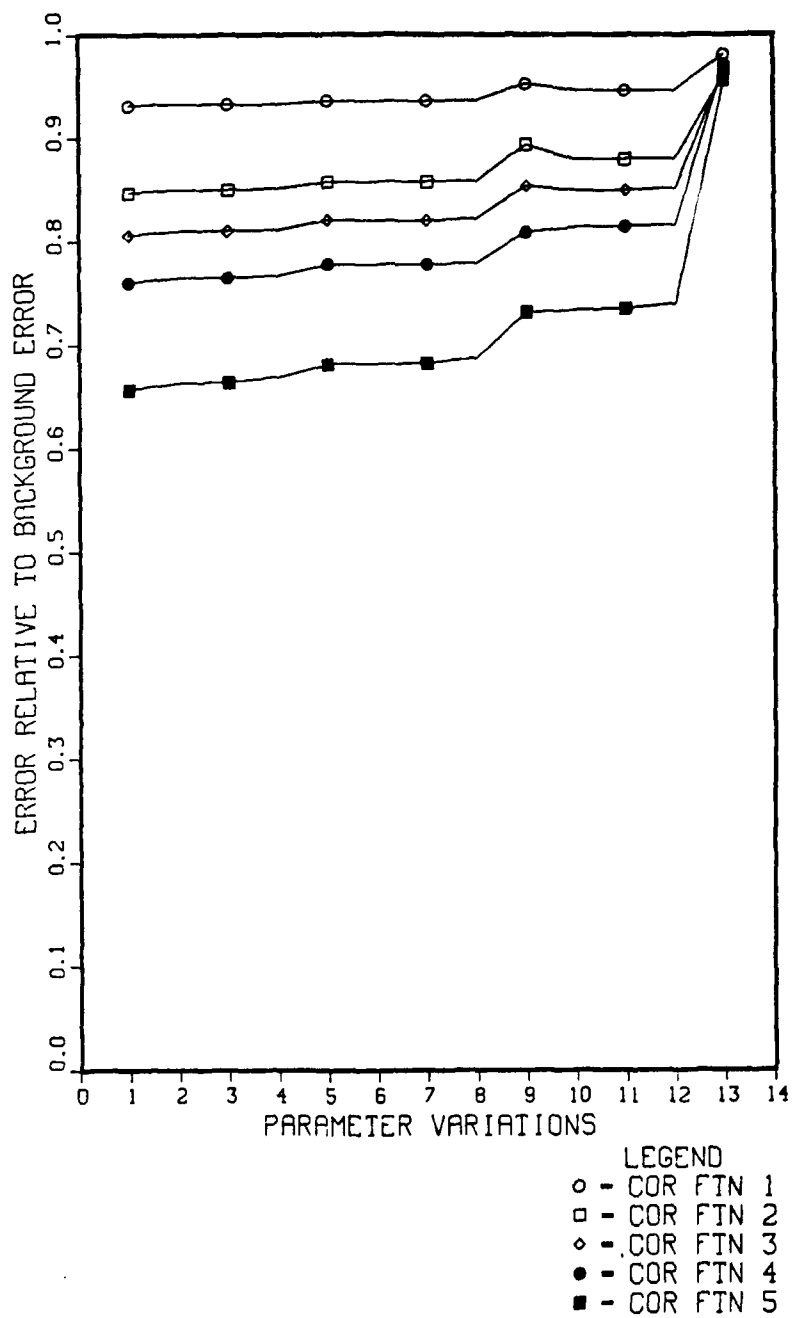
Figure 7: As in Figure 5, for the MA grid and observation set.
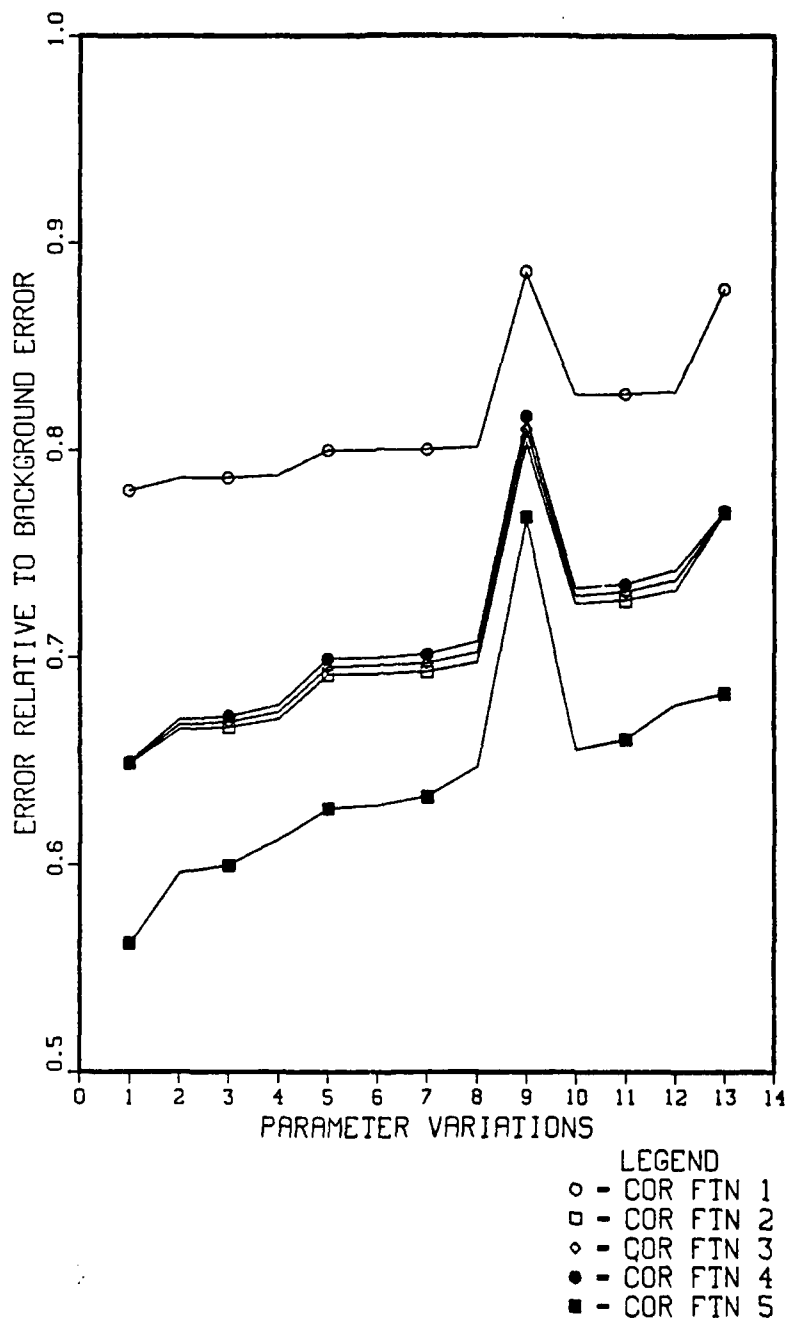
Figure 8: Expected error in OI wind analysis under various observation error and spatial correlation function conditions for the MUS grid and observation set.

OI WIND ERRORS, EC GRID
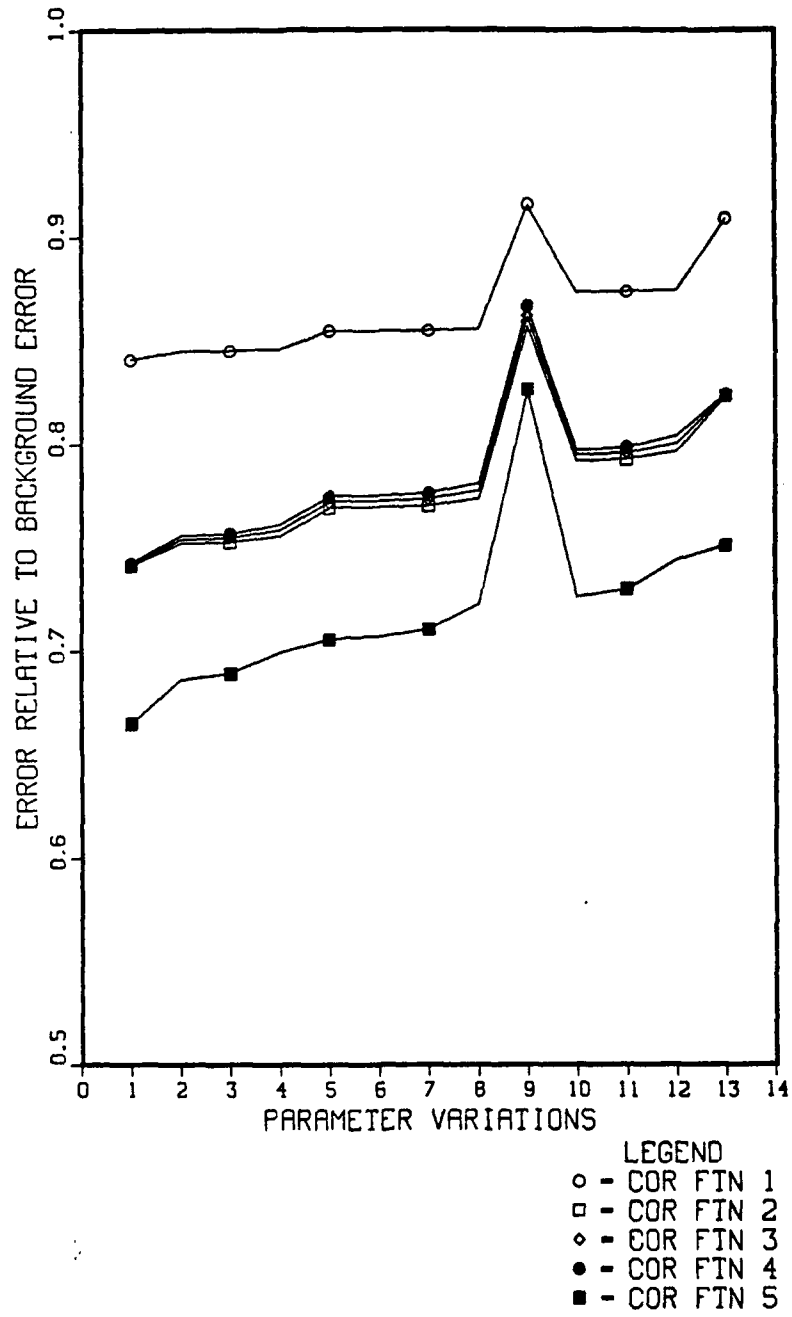
Figure 9: As in Figure 8, for the EC grid and observation set.

OI WIND ERRORS, MA GRID
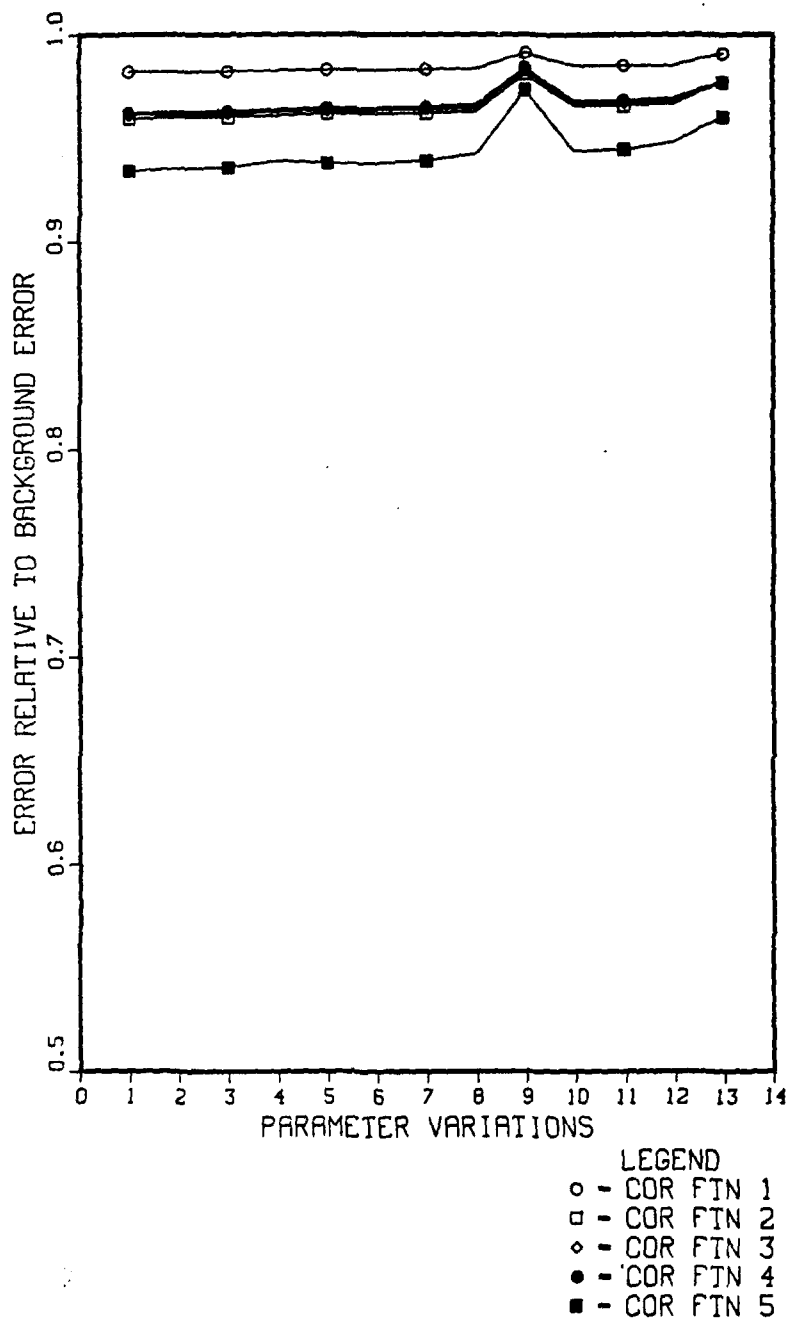
Figure 10: As in Figure 8, for the MA grid and observation set.
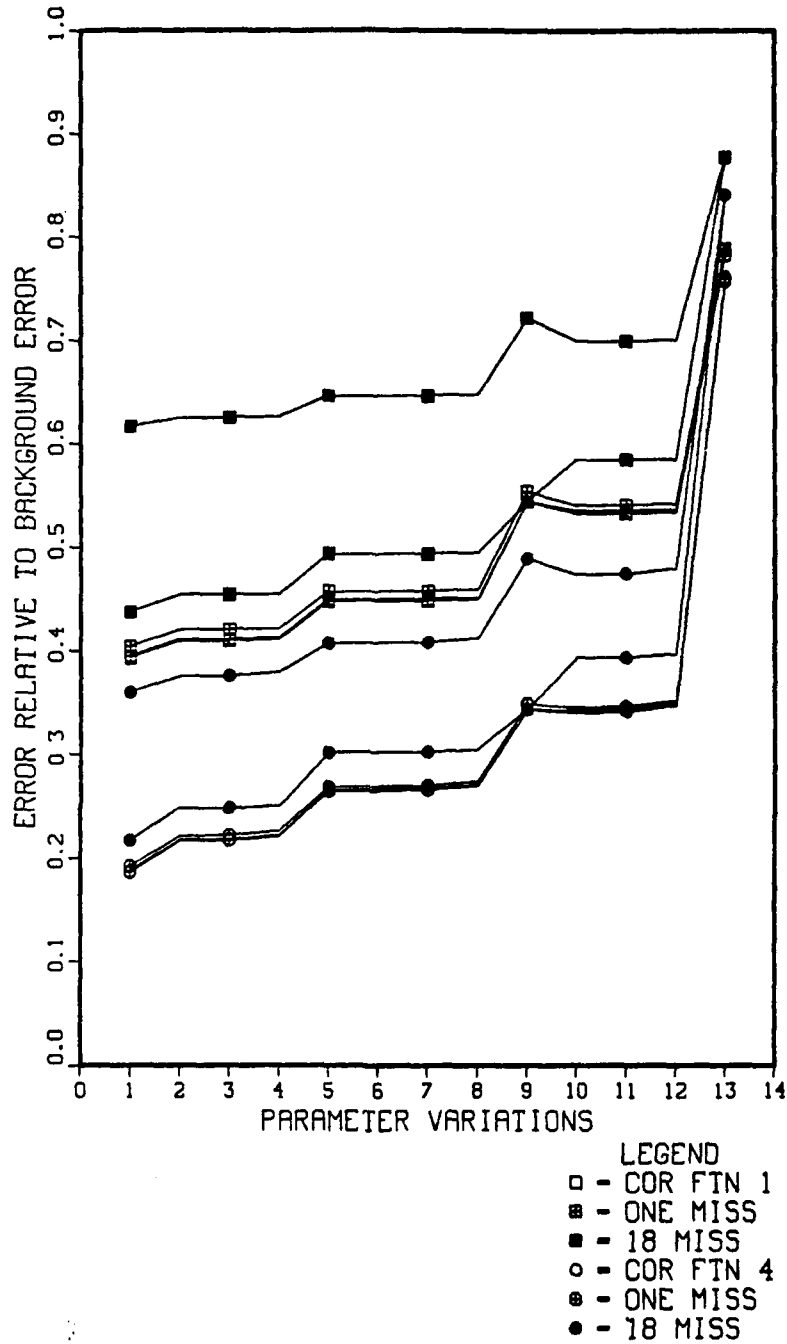
Figure 11: Expected error in OI height analysis under various observation error and spatial correlation function conditions for the MUS grid and observation set. The open square and circle mark the values for the entire observation set for correlation function numbers #1 and #4, respectively. The crossed square and circle mark two values; the lower for one missing wind observation, the upper one for both height and wind. The shaded square and circle mark two values; the lower one for 18 missing wind observations, the upper one for both heights and winds.
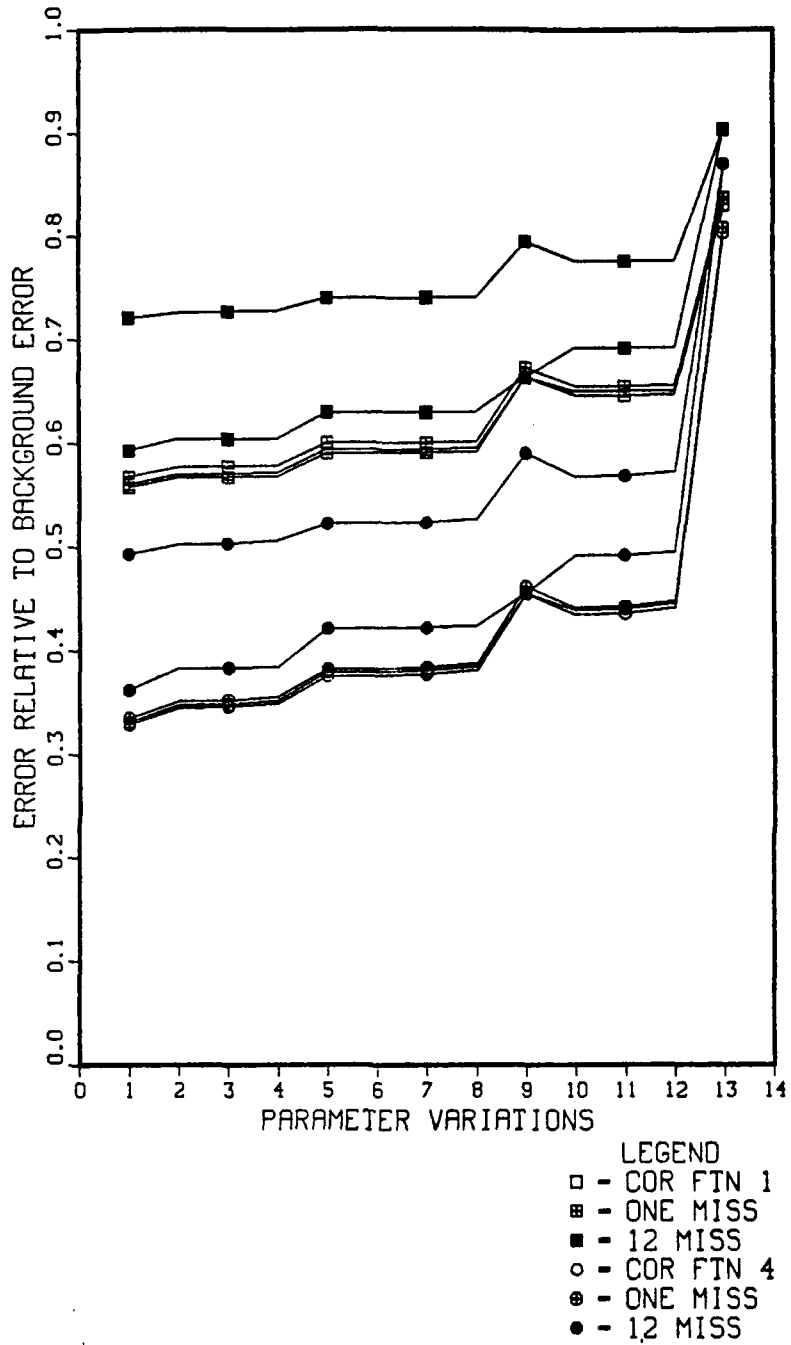
Figure 12: As in Figure 11, for EC grid and observation set, one and 12 missing observations.
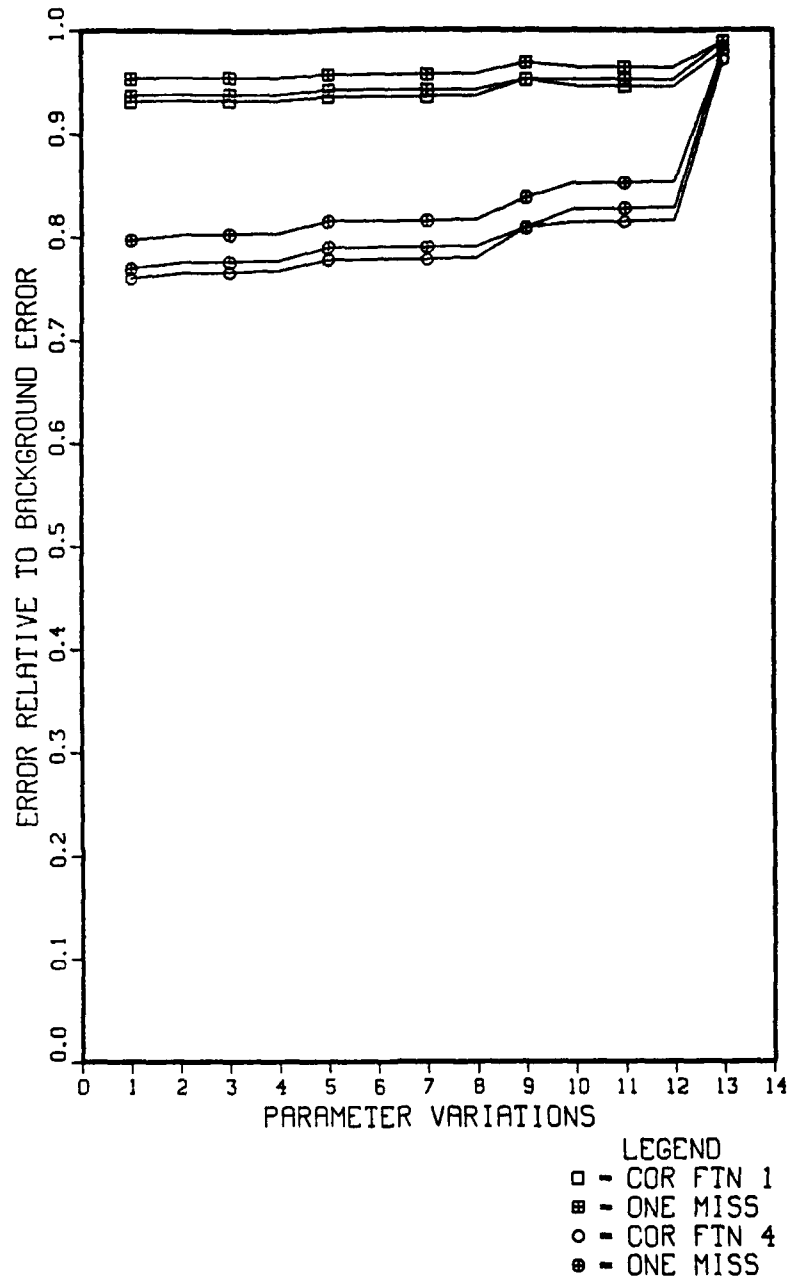
Figure 13: As in Figure 11, for **MA** grid and observation set, one missing observation (only).

OI W ERROR W/ MISSING OBS, MUS
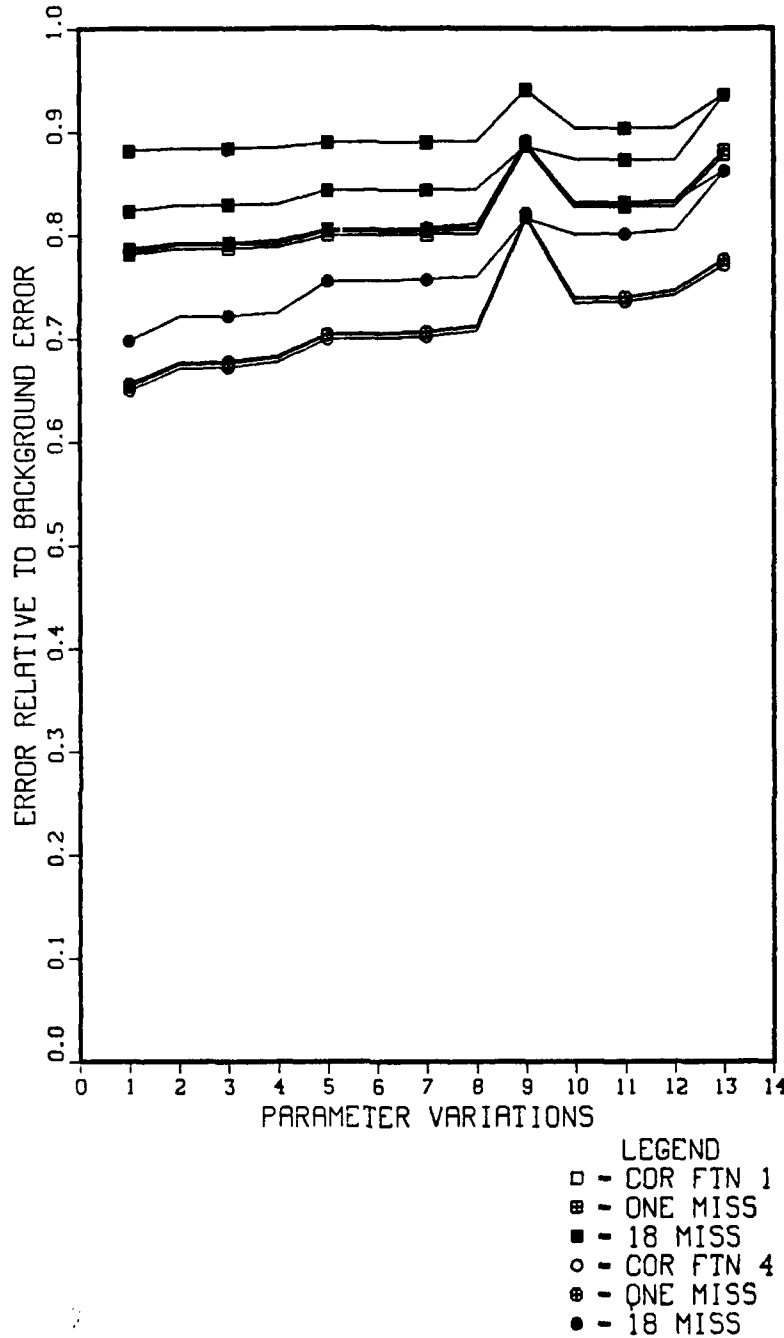
Figure 14: Expected error in OI wind analysis under various observation error and spatial correlation function conditions for the MUS grid and observation set. Symbols as in Figure 11.

OI W ERROR W/ MISSING OBS, EC
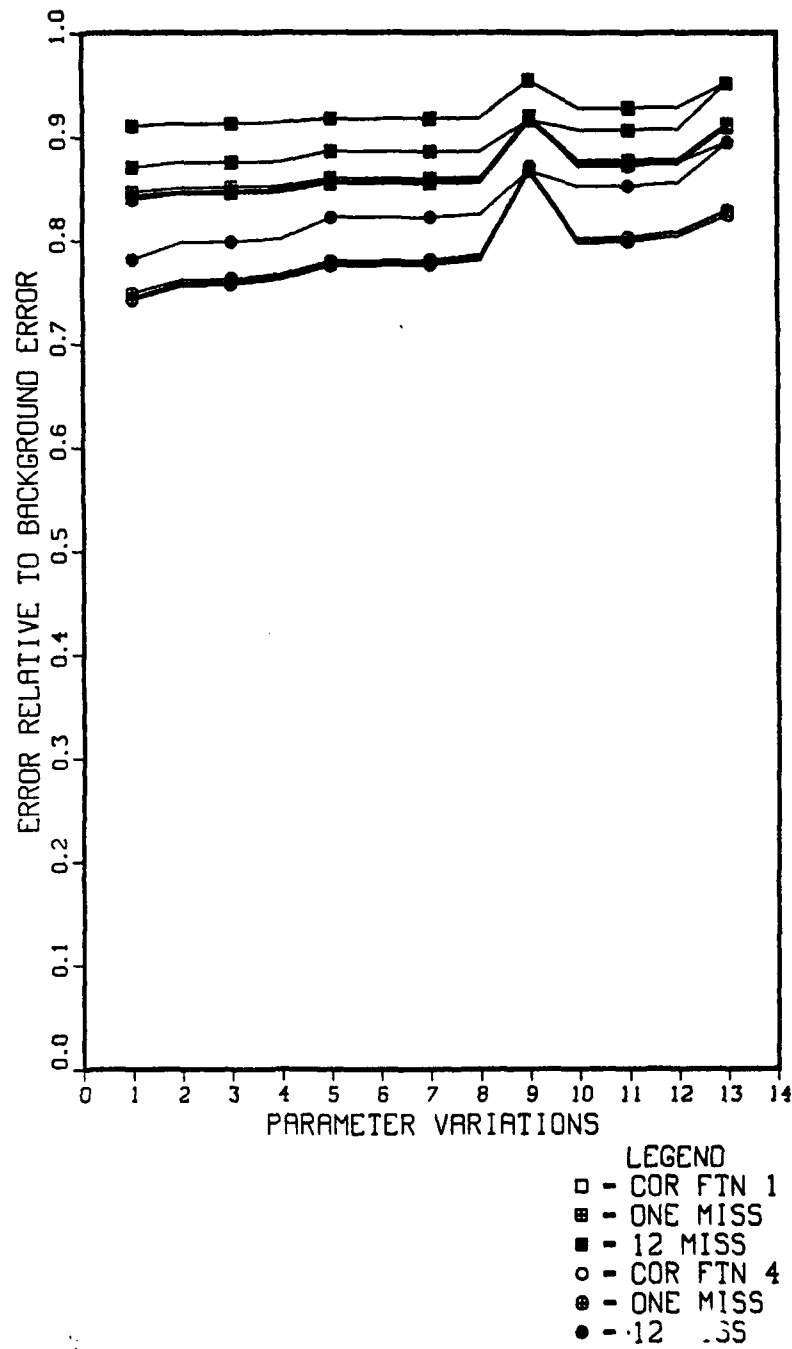
Figure 15: As in Figure 14, for EC grid and observation set, one and 12 missing observations.
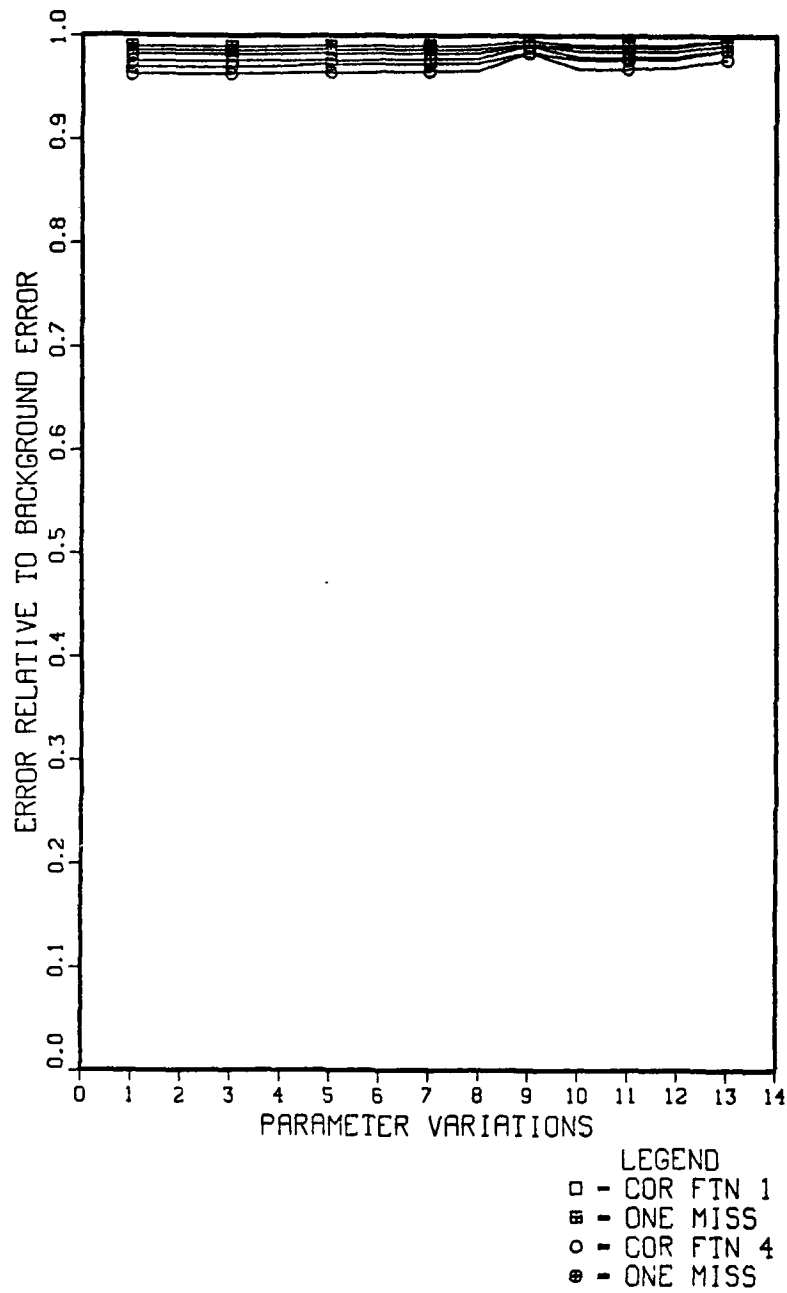
Figure 16: As in Figure 14, for MA grid and observation set, one missing observation (only).

HEIGHT SENSITIVITY PLOTS, MUS GRID
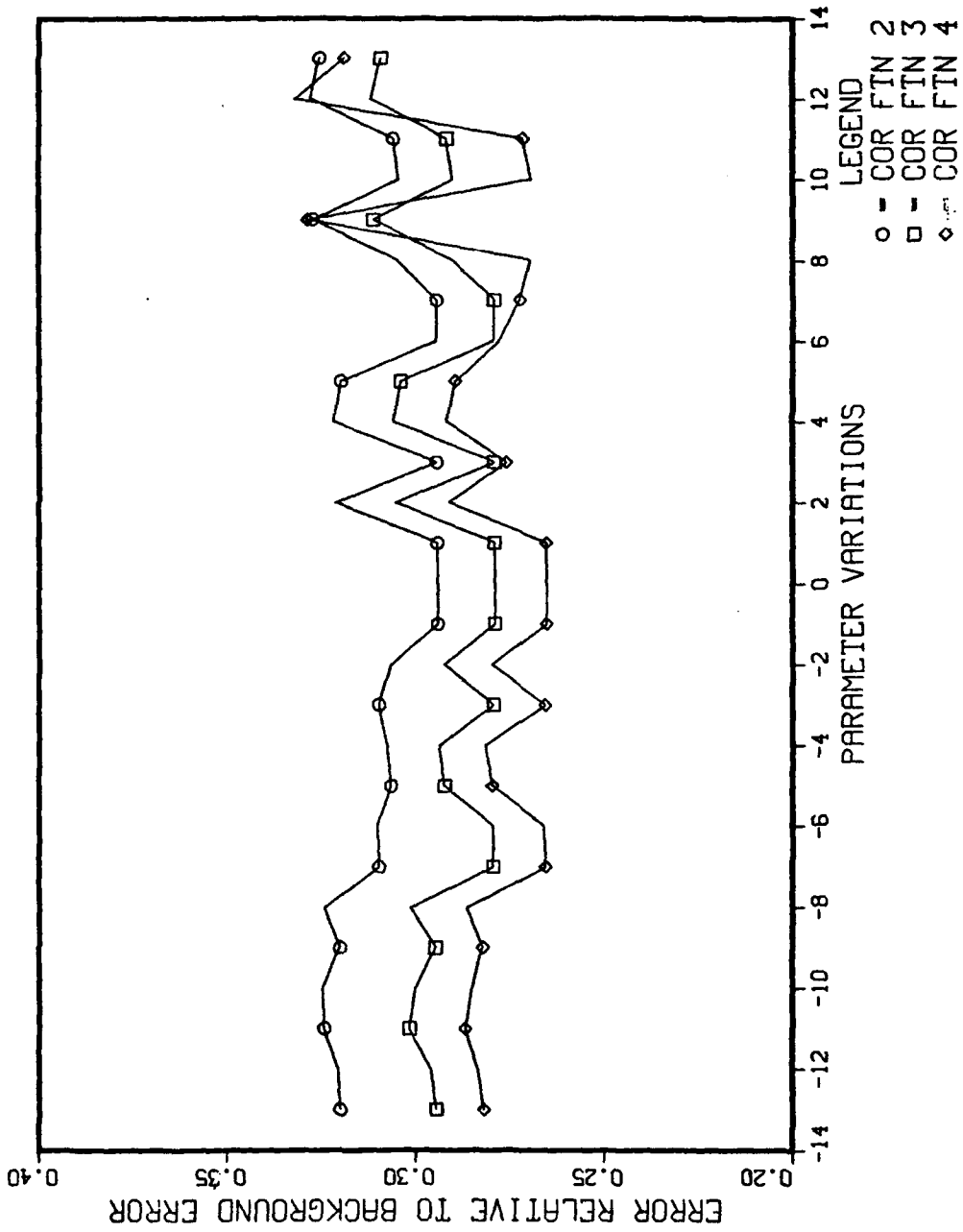
Figure 17: Expected error in the SI height analysis under various assumed correlation function and parameter values (see Table 4 for abscissae meanings), MUS grid and observation set.

34

Figure 18: As in Figure 17 for the EC grid and observation set.
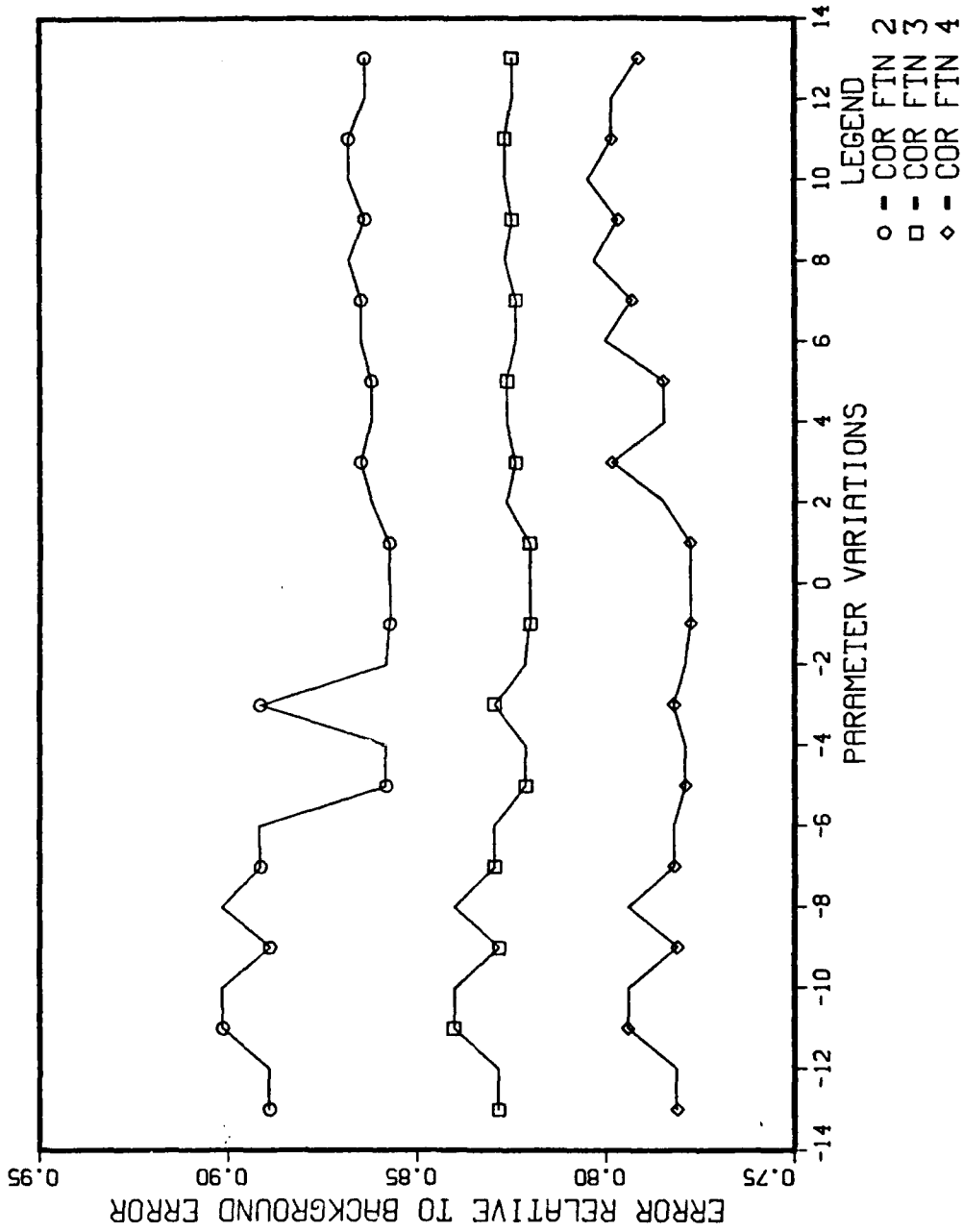
Figure 19: As in Figure 17 for the MA grid and observation set.
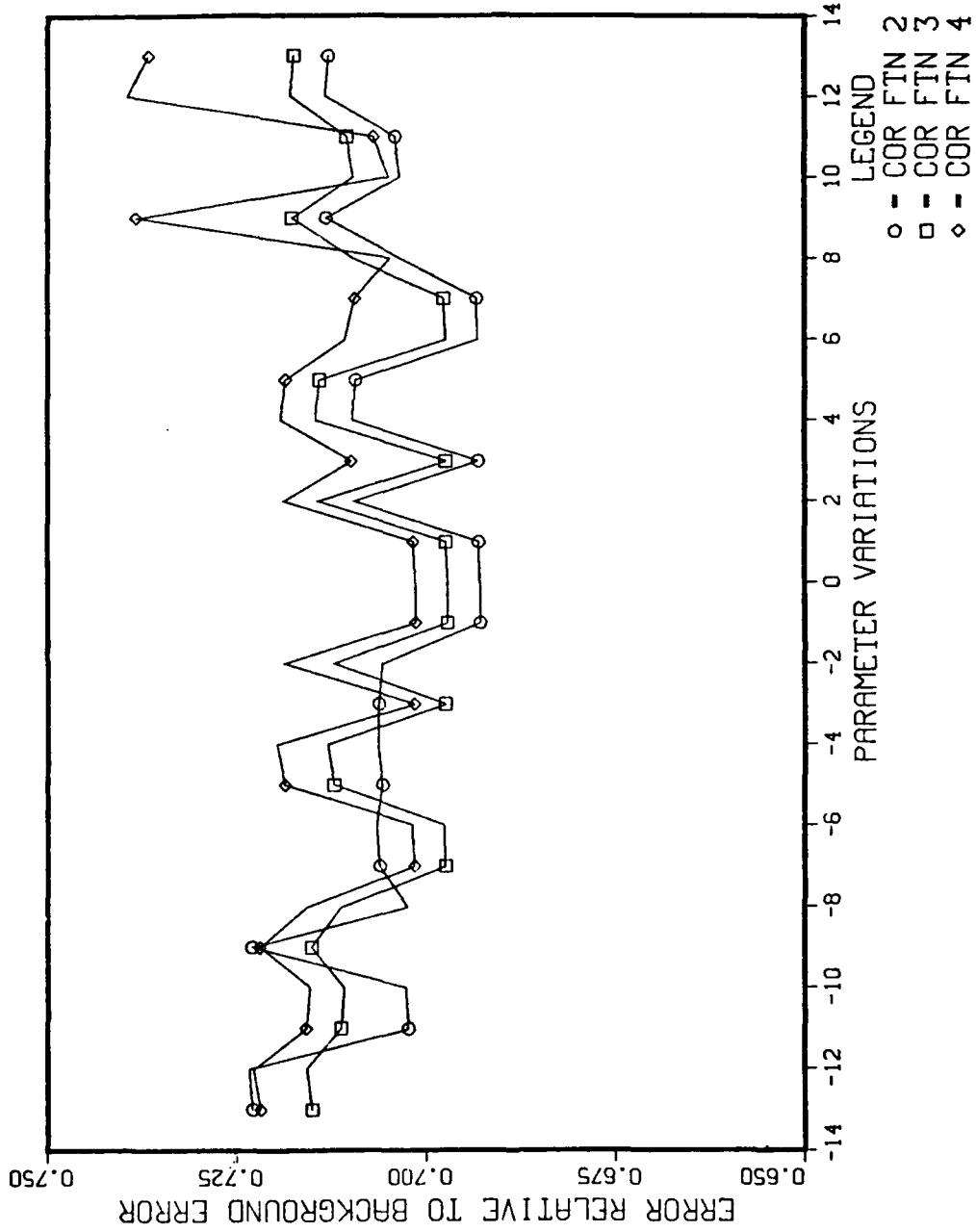
Figure 20: Expected error in the SI wind analysis under various assumed correlation function and parameter values (see Table 4 for abscissae meanings), MUS grid and observation set.

WIND SENSITIVITY PLOTS, EC GRID
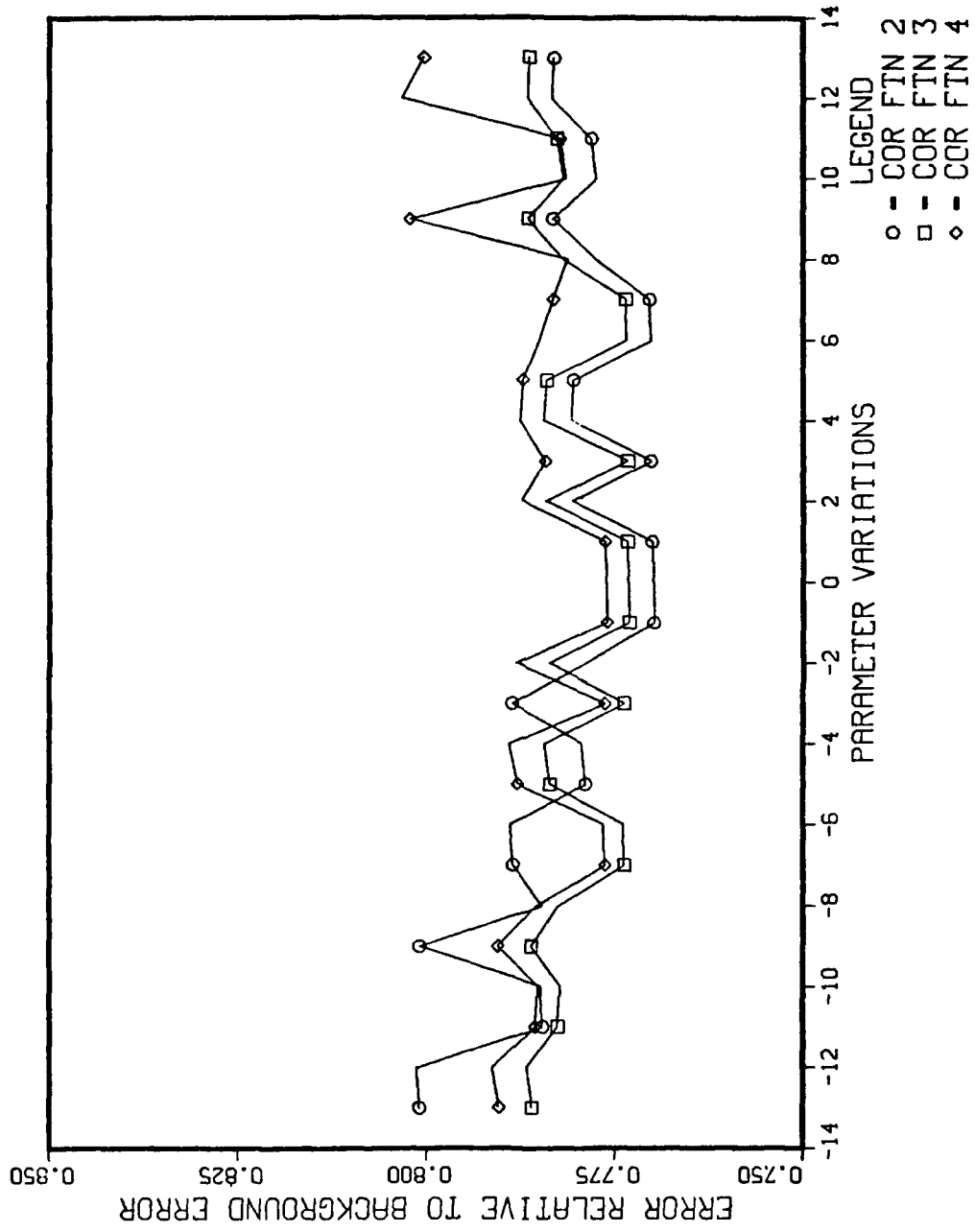
Figure 21: As in Figure 20 for the EC grid and observation set.

38
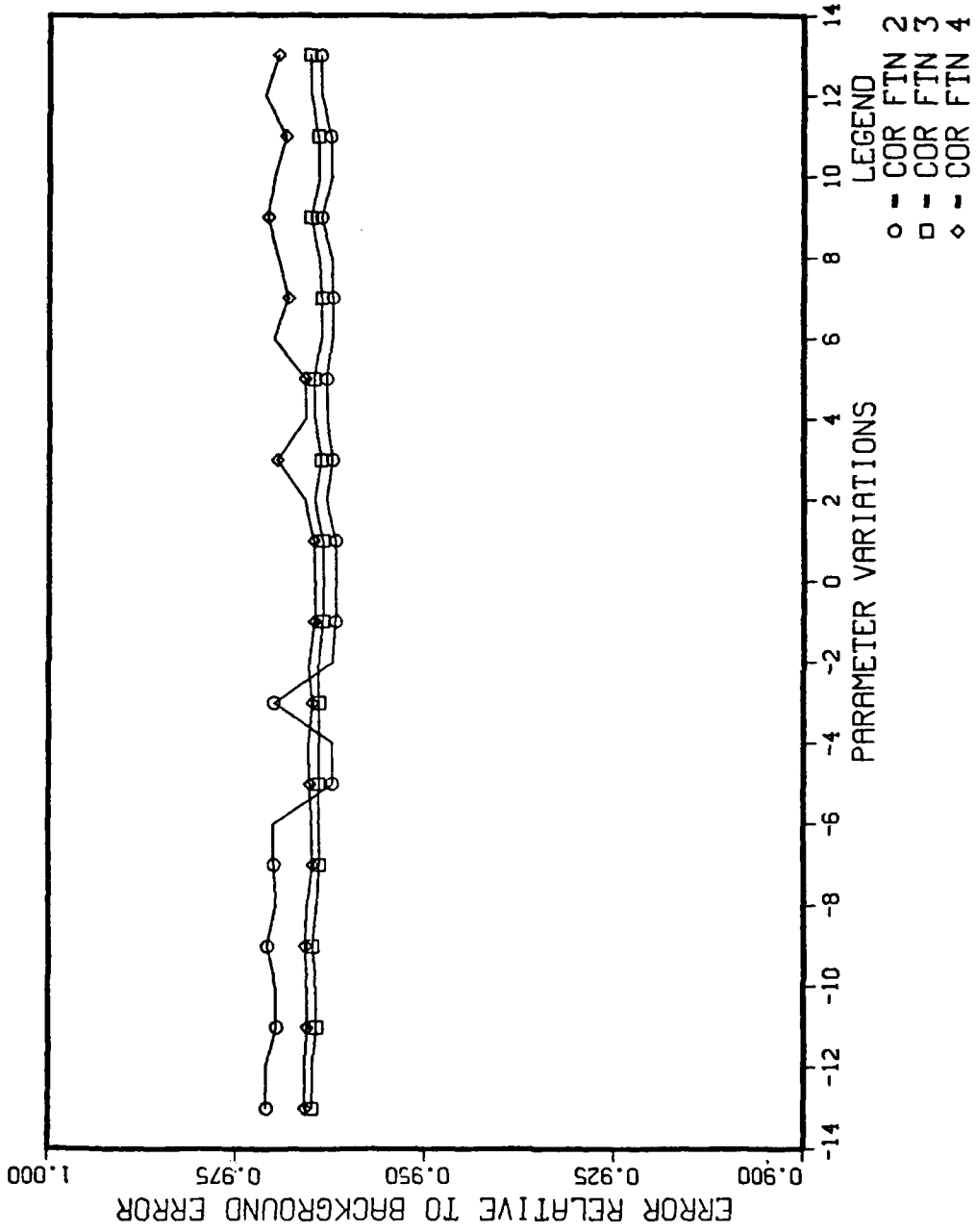
Figure 22: As in Figure 20 for the MA grid and observation set.

APPENDIX 1: TABLES

The tables giving the values plotted in the various figures, and some additional data as well, are given here. Most of the information is more readily accessible in the figures, however the tables are given for completeness.

The numbering scheme for the tables is a key to the grid and observation set and the correlation function number used. The experiment whose results are given by the tables follows:

Table 1.g.m: Expected error under various values of parameters in OI, nominal observation data.
- g - the grid used, 1 for MUS, 2 for EC, 3 for MA.
- m - the spatial correlation function number, 1-5.

Table 2.g.m: Expected error under various values of parameters in OI, wind observation missing at one point, as noted in text and Figures 1-3. g and m as in Table 1.g.m, except m=1 or 4.

Table 3.g.m: Expected error under various values of parameters in OI, height and wind observation missing at one point, as noted in text and Figures 1-3. g and m as in Table 1.g.m, except m=1 or 4.

Table 4.g.m: Expected error under various values of parameters in OI, wind observations missing at about one-half the observation points, as noted in text and Figures 1-3. g and m as in Table 1.g.m, except m=1 or 4.

Table 5.g.m: Expected error under various values of parameters in OI, height and wind observations missing at about one-half the observation points, as noted in text and Figures 1-3. g and m as in Table 1.g.m, except m=1 or 4.

Table 6.g.m-n: Expected error under various values of parameters in SI.
- g - the grid used, 1 for MUS, 2 for EC, 3 for MA.
- m - the true spatial correlation function number, 1-5.
- n - the assumed spatial correlation function number, 1-5, but not differing more than one from m.

40

Obs. error winds	Obs. error, heights 0.0	5.0	10.0	20.0	NoHeight
0.0			0.4474		
			0.8018		
			0.7978		
0.5		0.4090	0.4475	0.5321	
		0.7891	0.8019	0.8270	
		0.7834	0.7979	0.8263	
1.0	0.3927	0.4093	0.4478	0.5325	0.7828
	0.7835	0.7893	0.8022	0.8273	0.8739
	0.7771	0.7837	0.7982	0.8266	0.8814
2.0		0.4105	0.4491	0.5339	
		0.7905	0.8034	0.8285	
		0.7847	0.7992	0.8277	
NoWinds			0.5434		
			0.8911		
			0.8808		

Table 1.1.1: Expected error for observation accuracies

Obs. error winds	Obs. error, heights 0.0	5.0	10.0	20.0	NoHeight
0.0			0.2928		
			0.6920		
			0.6905		
0.5		0.2444	0.2931	0.3742	
		0.6674	0.6924	0.7240	
		0.6625	0.6908	0.7277	
1.0	0.2174	0.2452	0.2941	0.3754	0.6421
	0.6522	0.6685	0.6936	0.7253	0.7641
	0.6454	0.6636	0.6920	0.7289	0.7752
2.0		0.2483	0.2975	0.3800	
		0.6728	0.6981	0.7303	
		0.6677	0.6961	0.7336	
NoWinds			0.3794		
			0.8108		
			0.7970		

Table 1.1.2: Expected error for observation accuracies

Obs. error winds	Obs. error, heights 0.0	5.0	10.0	20.0	NoHeight
0.0			0.2775		
			0.6957		
			0.6947		
0.5		0.2291	0.2779	0.3560	
		0.6697	0.6962	0.7275	
		0.6651	0.6952	0.7318	
1.0	0.2007	0.2300	0.2789	0.3574	0.7078
	0.6525	0.6710	0.6976	0.7291	0.7645
	0.6457	0.6664	0.6965	0.7333	0.7755
2.0		0.2333	0.2827	0.3624	
		0.6760	0.7029	0.7350	
		0.6711	0.7014	0.7388	
NoWinds			0.3600		
			0.8169		
			0.8032		

Table 1.1.3: Expected error for observation accuracies

Obs. error winds	Obs. error, heights				
	0.0	5.0	10.0	20.0	NoHeight
0.0			0.2638		
			0.6994		
			0.6989		
0.5		0.2157	0.2642	0.3391	
		0.6721	0.6999	0.7307	
		0.6678	0.6994	0.7355	
1.0	0.1859	0.2166	0.2653	0.3406	0.7571
	0.6529	0.6737	0.7016	0.7326	0.7649
	0.6460	0.6692	0.7010	0.7373	0.7759
2.0		0.2202	0.2694	0.3462	
		0.6794	0.7077	0.7395	
		0.6746	0.7067	0.7437	
NoWinds			0.3427		
			0.8230		
			0.8095		

Table 1.1.4: Expected error for observation accuracies

Obs. error winds	Obs. error, heights				
	0.0	5.0	10.0	20.0	NoHeight
0.0			0.1983		
			0.6255		
			0.6283		
0.5		0.1549	0.1991	0.2591	
		0.5969	0.6271	0.6516	
		0.5946	0.6297	0.6589	
1.0	0.1183	0.1567	0.2015	0.2625	0.7283
	0.5653	0.6008	0.6315	0.6567	0.6772
	0.5583	0.5982	0.6338	0.6636	0.6879
2.0		0.1627	0.2095	0.2740	
		0.6138	0.6462	0.6740	
		0.6101	0.6474	0.6798	
NoWinds			0.2743		
			0.7753		
			0.7597		

Table 1.1.5: Expected error for observation accuracies

Obs. error winds	Obs. error, heights				
	0.0	5.0	10.0	20.0	NoHeight
0.0			0.5903		
			0.8543		
			0.8543		
0.5		0.5670	0.5904	0.6456	
		0.8435	0.8544	0.8747	
		0.8460	0.8544	0.8712	
1.0	0.5575	0.5672	0.5907	0.6459	0.8301
	0.8386	0.8437	0.8546	0.8749	0.9119
	0.8425	0.8462	0.8546	0.8714	0.9058
2.0		0.5681	0.5916	0.6471	
		0.8445	0.8554	0.8758	
		0.8470	0.8554	0.8723	
NoWinds			0.6631		
			0.9121		
			0.9190		

Table 1.2.1: Expected error for observation accuracies

Obs. error winds	Obs. error, heights				NoHeight
	0.0	5.0	10.0	20.0	
0.0			0.4266		
			0.7702		
			0.7671		
0.5		0.3972	0.4269	0.4854	
		0.7515	0.7705	0.7939	
		0.7516	0.7674	0.7886	
1.0	0.3828	0.3979	0.4277	0.4865	0.7146
	0.7392	0.7523	0.7713	0.7949	0.8255
	0.7426	0.7525	0.7683	0.7897	0.8202
2.0		0.4006	0.4310	0.4907	
		0.7554	0.7746	0.7987	
		0.7558	0.7718	0.7937	
NoWinds			0.5132		
			0.8544		
			0.8593		

Table 1.2.2: Expected error for observation accuracies

Obs. error winds	Obs. error, heights				NoHeight
	0.0	5.0	10.0	20.0	
0.0			0.3998		
			0.7733		
			0.7699		
0.5		0.3696	0.4001	0.4588	
		0.7537	0.7737	0.7969	
		0.7535	0.7703	0.7915	
1.0	0.3543	0.3703	0.4011	0.4600	0.7646
	0.7399	0.7546	0.7747	0.7980	0.8258
	0.7433	0.7546	0.7714	0.7928	0.8205
2.0		0.3733	0.4046	0.4647	
		0.7582	0.7786	0.8025	
		0.7584	0.7756	0.7975	
NoWinds			0.4824		
			0.8595		
			0.8640		

Table 1.2.3: Expected error for observation accuracies

Obs. error winds	Obs. error, heights				NoHeight
	0.0	5.0	10.0	20.0	
0.0			0.3753		
			0.7761		
			0.7724		
0.5		0.3445	0.3756	0.4336	
		0.7556	0.7765	0.7994	
		0.7552	0.7729	0.7940	
1.0	0.3284	0.3454	0.3767	0.4350	0.8030
	0.7402	0.7568	0.7778	0.8008	0.8262
	0.7437	0.7564	0.7742	0.7985	0.8209
2.0		0.3486	0.3806	0.4402	
		0.7609	0.7823	0.8061	
		0.7609	0.7790	0.8010	
NoWinds			0.4544		
			0.8643		
			0.8684		

Table 1.2.4: Expected error for observation accuracies

Obs. error winds	Obs. error, heights				NoHeight
	0.0	5.0	10.0	20.0	
0.0			0.2811		
			0.7072		
			0.7037		
0.5		0.2498	0.2819	0.3378	
		0.6865	0.7084	0.7277	
		0.6853	0.7050	0.7236	
1.0	0.2300	0.2517	0.2843	0.3410	0.7728
	0.6627	0.6895	0.7118	0.7316	0.7524
	0.6669	0.6884	0.7086	0.7277	0.7489
2.0		0.2580	0.2925	0.3519	
		0.6995	0.7234	0.7453	
		0.6990	0.7207	0.7417	
NoWinds			0.3686		
			0.8249		
			0.8274		

Table 1.2.5: Expected error for observation accuracies

Obs. error winds	Obs. error, heights				NoHeight
	0.0	5.0	10.0	20.0	
0.0			0.9355		
			0.9817		
			0.9843		
0.5		0.9320	0.9355	0.9454	
		0.9806	0.9817	0.9842	
		0.9837	0.9843	0.9859	
1.0	0.9307	0.9321	0.9356	0.9455	0.9807
	0.9802	0.9806	0.9817	0.9842	0.9903
	0.9835	0.9837	0.9843	0.9860	0.9914
2.0		0.9323	0.9358	0.9457	
		0.9808	0.9818	0.9843	
		0.9838	0.9844	0.9861	
NoWinds			0.9520		
			0.9896		
			0.9922		

Table 1.3.1: Expected error for observation accuracies

Obs. error winds	Obs. error, heights				NoHeight
	0.0	5.0	10.0	20.0	
0.0			0.8567		
			0.9585		
			0.9649		
0.5		0.8491	0.8569	0.8783	
		0.9561	0.9585	0.9631	
		0.9637	0.9649	0.9678	
1.0	0.8463	0.8494	0.8572	0.8787	0.9595
	0.9580	0.9562	0.9587	0.9633	0.9752
	0.9634	0.9639	0.9651	0.9680	0.9788
2.0		0.8508	0.8586	0.8801	
		0.9569	0.9594	0.9641	
		0.9646	0.9658	0.9687	
NoWinds			0.8934		
			0.9767		
			0.9846		

Table 1.3.2: Expected error for observation accuracies

Obs. error winds	Obs. error, heights				NoHeight
	0.0	5.0	10.0	20.0	
0.0			0.8196 0.9597 0.9668		
0.5		0.8094 0.9572 0.9657	0.8197 0.9598 0.9668	0.8486 0.9643 0.9694	
1.0	0.8058 0.9561 0.9655	0.8098 0.9574 0.9659	0.8201 0.9600 0.9670	0.8490 0.9645 0.9697	0.9657 0.9753 0.9788
2.0		0.8112 0.9582 0.9667	0.8216 0.9609 0.9678	0.8505 0.9654 0.9705	
NoWinds			0.8533 0.9783 0.9866		

Table 1.3.3: Expected error for observation accuracies

Obs. error winds	Obs. error, heights				NoHeight
	0.0	5.0	10.0	20.0	
0.0			0.7769 0.9607 0.9680		
0.5		0.7643 0.9580 0.9670	0.7770 0.9608 0.9681	0.8133 0.9652 0.9706	
1.0	0.7598 0.9567 0.9667	0.7647 0.9583 0.9672	0.7775 0.9610 0.9683	0.8137 0.9655 0.9709	0.9708 0.9753 0.9789
2.0		0.7662 0.9592 0.9681	0.7790 0.9620 0.9693	0.8152 0.9666 0.9718	
NoWinds			0.8084 0.9795 0.9880		

Table 1.3.4: Expected error for observation accuracies

Obs. error winds	Obs. error, heights				NoHeight
	0.0	5.0	10.0	20.0	
0.0			0.6806 0.9293 0.9457		
0.5		0.6626 0.9254 0.9444	0.6811 0.9296 0.9460	0.7332 0.9373 0.9497	
1.0	0.6565 0.9233 0.9444	0.6639 0.9263 0.9452	0.6824 0.9306 0.9468	0.7345 0.9383 0.9506	0.9552 0.9573 0.9632
2.0		0.6684 0.9294 0.9482	0.6870 0.9341 0.9499	0.7389 0.9420 0.9537	
NoWinds			0.7311 0.9642 0.9818		

Table 1.3.5: Expected error for observation accuracies

45

Obs. error winds	Obs. error, heights				NoHeight
	0.0	5.0	10.0	20.0	
0.0			0.4493 0.8064 0.8005		
0.5		0.4107 0.7935 0.7861	0.4494 0.8065 0.8006	0.5345 0.8317 0.8290	
1.0	0.3944 0.7879 0.7798	0.4110 0.7938 0.7864	0.4497 0.8067 0.8008	0.5349 0.8320 0.8293	0.7879 0.8794 0.8844
2.0		0.4123 0.7949 0.7874	0.4510 0.8078 0.8019	0.5363 0.8331 0.8303	
NoWinds			0.5434 0.8911 0.8805		

Table 2.1.1: Expected error for observation accuracies

Obs. error winds	Obs. error, heights				NoHeight
	0.0	5.0	10.0	20.0	
0.0			0.2652 0.7040 0.7018		
0.5		0.2167 0.6764 0.6706	0.2656 0.7045 0.7023	0.3414 0.7359 0.7386	
1.0	0.1868 0.6570 0.6487	0.2177 0.6779 0.6720	0.2667 0.7061 0.7038	0.3429 0.7377 0.7403	0.7604 0.7711 0.7797
2.0		0.2212 0.6834 0.6772	0.2708 0.7120 0.7094	0.3484 0.7444 0.7467	
NoWinds			0.3427 0.8230 0.8095		

Table 2.1.4: Expected error for observation accuracies

Obs. error winds	Obs. error, heights				NoHeight
	0.0	5.0	10.0	20.0	
0.0			0.5937 0.8556 0.8571		
0.5		0.5702 0.8448 0.8487	0.5938 0.8557 0.8571	0.6497 0.8761 0.8742	
1.0	0.5606 0.8399 0.8451	0.5704 0.8450 0.8489	0.5941 0.8559 0.8574	0.6500 0.8763 0.8745	0.8372 0.9138 0.9096
2.0		0.5713 0.8458 0.8497	0.5950 0.8567 0.8582	0.6511 0.8771 0.8753	
NoWinds			0.6631 0.9121 0.9190		

Table 2.2.1: Expected error for observation accuracies

Obs. error winds	Obs. error, heights				
	0.0	5.0	10.0	20.0	NoHeight
0.0			0.3788 0.7781 0.7762		
0.5		0.3474 0.7574 0.7585	0.3792 0.7785 0.7766	0.4384 0.8019 0.7984	
1.0	0.3306 0.7419 0.7467	0.3482 0.7585 0.7596	0.3802 0.7797 0.7779	0.4397 0.8033 0.7998	0.8087 0.8297 0.8264
2.0		0.3513 0.7626 0.7640	0.3840 0.7842 0.7826	0.4448 0.8085 0.8052	
NoWinds			0.4544 0.8643 0.8684		

Table 2.2.4: Expected error for observation accuracies

Obs. error winds	Obs. error, heights				
	0.0	5.0	10.0	20.0	NoHeight
0.0			0.9420 0.9864 0.9870		
0.5		0.9382 0.9854 0.9863	0.9421 0.9865 0.9870	0.9525 0.9891 0.9888	
1.0	0.9368 0.9850 0.9861	0.9383 0.9854 0.9863	0.9421 0.9865 0.9870	0.9525 0.9891 0.9888	0.9865 0.9957 0.9945
2.0		0.9384 0.9854 0.9864	0.9423 0.9865 0.9871	0.9527 0.9891 0.9889	
NoWinds			0.9520 0.9896 0.9922		

Table 2.3.1: Expected error for observation accuracies

Obs. error winds	Obs. error, heights				
	0.0	5.0	10.0	20.0	NoHeight
0.0			0.8143 0.9752 0.9772		
0.5		0.8014 0.9741 0.9765	0.8144 0.9753 0.9773	0.8515 0.9783 0.9795	
1.0	0.7968 0.9738 0.9764	0.8017 0.9743 0.9767	0.8148 0.9754 0.9775	0.8518 0.9785 0.9797	0.9805 0.9869 0.9862
2.0		0.8029 0.9749 0.9774	0.8160 0.9761 0.9782	0.8530 0.9792 0.9804	
NoWinds			0.8378 0.9887 0.9914		

Table 2.3.4: Expected error for observation accuracies

Obs. error winds	Obs. error, heights				NoHeight
	0.0	5.0	10.0	20.0	
0.0			0.4570 0.8065 0.8043		
0.5		0.4198 0.7941 0.7904	0.4571 0.8066 0.8044	0.5400 0.8310 0.8320	
1.0	0.4042 0.7888 0.7843	0.4202 0.7944 0.7906	0.4574 0.8069 0.8047	0.5404 0.8312 0.8323	0.7892 0.8772 0.8864
2.0		0.4214 0.7955 0.7917	0.4587 0.8080 0.8057	0.5418 0.8324 0.8333	
NoWinds			0.5534 0.8946 0.8842		

Table 3.1.1: Expected error for observation accuracies

Obs. error winds	Obs. error, heights				NoHeight
	0.0	5.0	10.0	20.0	
0.0			0.2681 0.7038 0.7047		
0.5		0.2207 0.6771 0.6744	0.2685 0.7043 0.7052	0.3439 0.7348 0.7411	
1.0	0.1919 0.6585 0.6533	0.2217 0.6787 0.6758	0.2697 0.7059 0.7067	0.3454 0.7366 0.7428	0.7616 0.7698 0.7819
2.0		0.2253 0.6844 0.6811	0.2738 0.7120 0.7123	0.3509 0.7435 0.7490	
NoWinds			0.3482 0.8266 0.8133		

Table 3.1.4: Expected error for observation accuracies

Obs. error winds	Obs. error, heights				NoHeight
	0.0	5.0	10.0	20.0	
0.0			0.6000 0.8595 0.8592		
0.5		0.5771 0.8496 0.8512	0.6001 0.8596 0.8593	0.6544 0.8784 0.8756	
1.0	0.5678 0.8452 0.8478	0.5773 0.8498 0.8514	0.6003 0.8598 0.8595	0.6547 0.8786 0.8758	0.8372 0.9138 0.9096
2.0		0.5782 0.8506 0.8522	0.6013 0.8606 0.8603	0.6558 0.8794 0.8767	
NoWinds			0.6723 0.9166 0.9221		

Table 3.2.1: Expected error for observation accuracies

Obs. error winds	Obs. error, heights 0.0	5.0	10.0	20.0	NoHeight
0.0			0.3816		
			0.7805		
			0.7778		
0.5		0.3509	0.3820	0.4406	
		0.7614	0.7809	0.8029	
		0.7609	0.7782	0.7991	
1.0	0.3348	0.3518	0.3831	0.4420	0.8087
	0.7474	0.7625	0.7821	0.8043	0.8297
	0.7498	0.7621	0.7795	0.8006	0.8264
2.0		0.3550	0.3870	0.4472	
		0.7667	0.7867	0.8096	
		0.7665	0.7843	0.8060	
NoWinds			0.4611		
			0.8689		
			0.8721		

Table 3.2.4:   Expected error for observation accuracies

Obs. error winds	Obs. error, heights 0.0	5.0	10.0	20.0	NoHeight
0.0			0.9569		
			0.9902		
			0.9896		
0.5		0.9543	0.9569	0.9643	
		0.9897	0.9902	0.9914	
		0.9892	0.9896	0.9908	
1.0	0.9534	0.9544	0.9570	0.9643	0.9885
	0.9896	0.9897	0.9902	0.9915	0.9957
	0.9891	0.9893	0.9896	0.9908	0.9945
2.0		0.9545	0.9572	0.9645	
		0.9898	0.9902	0.9915	
		0.9893	0.9897	0.9909	
NoWinds			0.9688		
			0.9945		
			0.9951		

Table 3.3.1:   Expected error for observation accuracies

Obs. error winds	Obs. error, heights 0.0	5.0	10.0	20.0	NoHeight
0.0			0.7889		
			0.9695		
			0.9747		
0.5		0.7747	0.7890	0.8264	
		0.9659	0.9695	0.9755	
		0.9732	0.9747	0.9777	
1.0	0.7691	0.7750	0.7893	0.8267	0.9805
	0.9642	0.9661	0.9697	0.9757	0.9869
	0.9727	0.9734	0.9749	0.9779	0.9862
2.0		0.7761	0.7903	0.8277	
		0.9666	0.9702	0.9762	
		0.9741	0.9756	0.9786	
NoWinds			0.8084		
			0.9795		
			0.9880		

Table 3.3.4:   Expected error for observation accuracies

Obs. error winds	Obs. error, heights				NoHeight
	0.0	5.0	10.0	20.0	
0.0			0.4933		
			0.8457		
			0.8406		
0.5		0.4540	0.4933	0.5838	
		0.8321	0.8457	0.8734	
		0.8253	0.8407	0.8720	
1.0	0.4377	0.4542	0.4935	0.5840	0.8774
	0.8262	0.8322	0.8459	0.8735	0.9305
	0.8187	0.8255	0.8408	0.8721	0.9399
2.0		0.4548	0.4942	0.5848	
		0.8328	0.8465	0.8741	
		0.8260	0.8413	0.8727	
NoWinds			0.5434		
			0.8911		
			0.8808		

Table 4.1.1: Expected error for observation accuracies

Obs. error winds	Obs. error, heights				NoHeight
	0.0	5.0	10.0	20.0	
0.0			0.3014		
			0.7570		
			0.7534		
0.5		0.2477	0.3016	0.3920	
		0.7244	0.7573	0.7983	
		0.7167	0.7537	0.8016	
1.0	0.2167	0.2482	0.3022	0.3929	0.8412
	0.7026	0.7253	0.7583	0.7994	0.8541
	0.6924	0.7175	0.7545	0.8025	0.8688
2.0		0.2500	0.3045	0.3962	
		0.7285	0.7617	0.8035	
		0.7202	0.7574	0.8060	
NoWinds			0.3427		
			0.8230		
			0.8095		

Table 4.1.4: Expected error for observation accuracies

Obs. error winds	Obs. error, heights				NoHeight
	0.0	5.0	10.0	20.0	
0.0			0.6297		
			0.8847		
			0.8860		
0.5		0.6038	0.6297	0.6918	
		0.8731	0.8847	0.9076	
		0.8768	0.8860	0.9053	
1.0	0.5932	0.6039	0.6298	0.6916	0.9039
	0.8679	0.8732	0.8848	0.9077	0.9537
	0.8729	0.8769	0.8862	0.9054	0.9481
2.0		0.6043	0.6303	0.6922	
		0.8735	0.8852	0.9081	
		0.8774	0.8866	0.9059	
NoWinds			0.6632		
			0.9121		
			0.9190		

Table 4.2.1: Expected error for observation accuracies

Obs. error	Obs. error, heights				
winds	0.0	5.0	10.0	20.0	NoHeight
0.0			0.4211 0.8237 0.8191		
0.5		0.3826 0.7977 0.7970	0.4212 0.8239 0.8193	0.4911 0.8555 0.8483	
1.0	0.3617 0.7796 0.7826	0.3830 0.7982 0.7976	0.4217 0.8245 0.8200	0.4918 0.8562 0.8491	0.8703 0.8978 0.8897
2.0		0.3843 0.8003 0.7999	0.4234 0.8268 0.8226	0.4945 0.8590 0.8522	
NoWinds			0.4544 0.8643 0.8684		

Table 4.2.4: Expected error for observation accuracies

51

Obs. error winds	Obs. error, heights				NoHeight
	0.0	5.0	10.0	20.0	
0.0			0.6457		
			0.8893		
			0.8900		
0.5		0.6247	0.6458	0.6989	
		0.8831	0.8894	0.9024	
		0.8838	0.8901	0.9042	
1.0	0.6166	0.6250	0.6461	0.6991	0.8774
	0.8806	0.8833	0.8895	0.9026	0.9305
	0.8814	0.8840	0.8902	0.9043	0.9399
2.0		0.6258	0.6470	0.7001	
		0.8839	0.8902	0.9033	
		0.8845	0.8908	0.9049	
NoWinds			0.7214		
			0.9415		
			0.9390		

Table 5.1.1: Expected error for observation accuracies

Obs. error winds	Obs. error, heights				NoHeight
	0.0	5.0	10.0	20.0	
0.0			0.4067		
			0.8070		
			0.8035		
0.5		0.3747	0.4070	0.4729	
		0.7926	0.8074	0.8263	
		0.7875	0.8039	0.8289	
1.0	0.3595	0.3756	0.4080	0.4741	0.8412
	0.7838	0.7936	0.8085	0.8275	0.8541
	0.7789	0.7885	0.8049	0.8300	0.8688
2.0		0.3789	0.4118	0.4787	
		0.7975	0.8126	0.8322	
		0.7920	0.8085	0.8340	
NoWinds			0.4887		
			0.8949		
			0.8862		

Table 5.1.4: Expected error for observation accuracies

Obs. error winds	Obs. error, heights				NoHeight
	0.0	5.0	10.0	20.0	
0.0			0.7397		
			0.9175		
			0.9164		
0.5		0.7260	0.7398	0.7753	
		0.9123	0.9175	0.9286	
		0.9121	0.9164	0.9260	
1.0	0.7207	0.7262	0.7400	0.7755	0.9039
	0.9103	0.9125	0.9177	0.9287	0.9537
	0.9103	0.9122	0.9166	0.9261	0.9481
2.0		0.7268	0.7406	0.7762	
		0.9129	0.9181	0.9292	
		0.9127	0.9171	0.9266	
NoWinds			0.7946		
			0.9523		
			0.9558		

Table 5.2.1: Expected error for observation accuracies

Obs. error winds	Obs. error, heights				
	0.0	5.0	10.0	20.0	NoHeight
0.0			0.5221		
			0.8580		
			0.8540		
0.5		0.5022	0.5224	0.5674	
		0.8465	0.8582	0.8738	
		0.8440	0.8543	0.8682	
1.0	0.4931	0.5028	0.5232	0.5684	0.8703
	0.8396	0.8472	0.8590	0.8746	0.8978
	0.8382	0.8448	0.8552	0.8691	0.8897
2.0		0.5054	0.5262	0.5722	
		0.8498	0.8618	0.8779	
		0.8477	0.8583	0.8727	
NoWinds			0.5899		
			0.9181		
			0.9214		

Table 5.2.4: Expected error for observation accuracies

Assmd Obs. err, winds	Assumed Obs. error, heights		
	5.0	10.0	20.0
0.5	0.4531	0.4478	0.4717
	0.8052	0.8022	0.8118
	0.8015	0.7982	0.8087
1.0	0.4531	0.4478	0.4716
	0.8052	0.8022	0.8117
	0.8015	0.7982	0.8087
2.0	0.4532	0.4478	0.4713
	0.8052	0.8022	0.8117
	0.8015	0.7982	0.8087

Table 6.1.1-1: Variation of expected error

Assmd Obs. err, winds	Assumed Obs. error, heights		
	5.0	10.0	20.0
0.5	0.3045	0.2945	0.3279
	0.7038	0.6939	0.7127
	0.7030	0.6923	0.7139
1.0	0.3047	0.2944	0.3273
	0.7039	0.6939	0.7126
	0.7031	0.6922	0.7137
2.0	0.3059	0.2944	0.3255
	0.7045	0.6941	0.7123
	0.7037	0.6924	0.7134

Table 6.1.2-3: Variation of expected error

Assmd Obs. err, winds	Assumed Obs. error, heights		
	5.0	10.0	20.0
0.5	0.4583	0.4709	0.5476
	0.8064	0.8120	0.8379
	0.8020	0.8081	0.8371
1.0	0.4580	0.4699	0.5457
	0.8061	0.8116	0.8374
	0.8017	0.8077	0.8366
2.0	0.4568	0.4666	0.5387
	0.8054	0.8105	0.8356
	0.8011	0.8067	0.8349

Table 6.1.1-2: Variation of expected error

Assmd Obs. err, winds	Assumed Obs. error, heights		
	5.0	10.0	20.0
0.5	0.2945	0.2793	0.3016
	0.7149	0.6980	0.7108
	0.7152	0.6968	0.7116
1.0	0.2947	0.2793	0.3012
	0.7150	0.6980	0.7107
	0.7153	0.6968	0.7115
2.0	0.2958	0.2796	0.2999
	0.7156	0.6982	0.7104
	0.7159	0.6971	0.7112

Table 6.1.3-2: Variation of expected error

Assmd Obs. err, winds	Assumed Obs. error, heights		
	5.0	10.0	20.0
0.5	0.3200	0.3096	0.3242
	0.7226	0.7068	0.7032
	0.7232	0.7054	0.7014
1.0	0.3201	0.3097	0.3243
	0.7227	0.7069	0.7033
	0.7233	0.7055	0.7015
2.0	0.3205	0.3101	0.3247
	0.7230	0.7073	0.7036
	0.7235	0.7058	0.7018

Table 6.1.2-1: Variation of expected error

Assmd Obs. err, winds	Assumed Obs. error, heights		
	5.0	10.0	20.0
0.5	0.2922	0.2789	0.3059
	0.7121	0.6977	0.7139
	0.7122	0.6965	0.7152
1.0	0.2925	0.2789	0.3054
	0.7122	0.6976	0.7137
	0.7123	0.6965	0.7150
2.0	0.2937	0.2791	0.3038
	0.7129	0.6979	0.7134
	0.7130	0.6967	0.7147

Table 6.1.3-3: Variation of expected error

Assmd Obs. err, winds	Assumed Obs. error, heights		
	5.0	10.0	20.0
0.5	0.3064	0.2941	0.3217
	0.7060	0.6936	0.7094
	0.7054	0.6920	0.7100
1.0	0.3066	0.2941	0.3212
	0.7060	0.6936	0.7093
	0.7055	0.6920	0.7099
2.0	0.3076	0.2942	0.3197
	0.7066	0.6938	0.7090
	0.7060	0.6921	0.7096

Table 6.1.2-2: Variation of expected error

Assmd Obs. err, winds	Assumed Obs. error, heights		
	5.0	10.0	20.0
0.5	0.2901	0.2793	0.3118
	0.7096	0.6979	0.7170
	0.7095	0.6968	0.7188
1.0	0.2904	0.2792	0.3112
	0.7097	0.6979	0.7168
	0.7096	0.6968	0.7186
2.0	0.2918	0.2792	0.3092
	0.7106	0.6982	0.7165
	0.7104	0.6970	0.7183

Table 6.1.3-4: Variation of expected error

Assmd Obs. err, winds	Assumed Obs. error, heights		
	5.0	10.0	20.0
0.5	0.2819	0.2655	0.2868
	0.7213	0.7018	0.7151
	0.7224	0.7013	0.7166
1.0	0.2822	0.2656	0.2864
	0.7214	0.7018	0.7150
	0.7225	0.7012	0.7164
2.0	0.2835	0.2659	0.2850
	0.7222	0.7021	0.7147
	0.7232	0.7015	0.7161

Table 6.1.4-3: Variation of expected error

Assmd Obs. err, winds	Assumed Obs. error, heights		
	5.0	10.0	20.0
0.5	0.2187	0.2016	0.2237
	0.6587	0.6316	0.6467
	0.6640	0.6339	0.6517
1.0	0.2198	0.2015	0.2224
	0.6595	0.6315	0.6461
	0.6647	0.6338	0.6511
2.0	0.2242	0.2024	0.2192
	0.6645	0.6331	0.6462
	0.6694	0.6354	0.6511

Table 6.1.5-5: Variation of expected error

Assmd Obs. err, winds	Assumed Obs. error, heights		
	5.0	10.0	20.0
0.5	0.2796	0.2653	0.2917
	0.7182	0.7016	0.7181
	0.7190	0.7010	0.7200
1.0	0.2799	0.2653	0.2912
	0.7184	0.7016	0.7179
	0.7192	0.7010	0.7198
2.0	0.2814	0.2655	0.2894
	0.7193	0.7019	0.7176
	0.7201	0.7013	0.7195

Table 6.1.4-4: Variation of expected error

Assmd Obs. err, winds	Assumed Obs. error, heights		
	5.0	10.0	20.0
0.5	0.5939	0.5907	0.6057
	0.8574	0.8546	0.8626
	0.8564	0.8546	0.8608
1.0	0.5940	0.5907	0.6056
	0.8574	0.8546	0.8626
	0.8564	0.8546	0.8607
2.0	0.5941	0.5907	0.6054
	0.8574	0.8546	0.8626
	0.8565	0.8546	0.8607

Table 6.2.1-1: Variation of expected error

Assmd Obs. err, winds	Assumed Obs. error, heights		
	5.0	10.0	20.0
0.5	0.2693	0.2777	0.3320
	0.7051	0.7105	0.7369
	0.7046	0.7107	0.7420
1.0	0.2695	0.2760	0.3287
	0.7050	0.7097	0.7358
	0.7046	0.7100	0.7408
2.0	0.2716	0.2724	0.3190
	0.7072	0.7092	0.7341
	0.7067	0.7095	0.7391

Table 6.1.4-5: Variation of expected error

Assmd Obs. err, winds	Assumed Obs. error, heights		
	5.0	10.0	20.0
0.5	0.6311	0.6368	0.6817
	0.8631	0.8681	0.8884
	0.8627	0.8663	0.8832
1.0	0.6304	0.6356	0.6797
	0.8628	0.8677	0.8879
	0.8625	0.8659	0.8827
2.0	0.6279	0.6313	0.6725
	0.8620	0.8665	0.8863
	0.8617	0.8647	0.8810

Table 6.2.1-2: Variation of expected error

Assmd Obs. err, winds	Assumed Obs. error, heights		
	5.0	10.0	20.0
0.5	0.2383	0.2095	0.2117
	0.7005	0.6431	0.6370
	0.7084	0.6465	0.6398
1.0	0.2388	0.2099	0.2117
	0.7009	0.6434	0.6371
	0.7088	0.6468	0.6399
2.0	0.2408	0.2113	0.2120
	0.7029	0.6448	0.6377
	0.7106	0.6481	0.6404

Table 6.1.5-4: Variation of expected error

Assmd Obs. err, winds	Assumed Obs. error, heights		
	5.0	10.0	20.0
0.5	0.4682	0.4655	0.4823
	0.8059	0.7913	0.7865
	0.7957	0.7857	0.7826
1.0	0.4683	0.4656	0.4824
	0.8060	0.7913	0.7865
	0.7957	0.7858	0.7826
2.0	0.4689	0.4661	0.4830
	0.8063	0.7916	0.7868
	0.7961	0.7861	0.7829

Table 6.2.2-1: Variation of expected error

Assmd Obs. err, winds	Assumed Obs. error, heights 5.0	10.0	20.0
0.5	0.4351	0.4278	0.4458
	0.7818	0.7713	0.7830
	0.7759	0.7683	0.7785
1.0	0.4353	0.4277	0.4455
	0.7818	0.7713	0.7829
	0.7760	0.7683	0.7784
2.0	0.4362	0.4279	0.4445
	0.7823	0.7715	0.7827
	0.7765	0.7685	0.7782

Table 6.2.2-2: Variation of expected error

Assmd Obs. err, winds	Assumed Obs. error, heights 5.0	10.0	20.0
0.5	0.4081	0.4015	0.4230
	0.7846	0.7750	0.7890
	0.7788	0.7717	0.7841
1.0	0.4084	0.4014	0.4226
	0.7847	0.7749	0.7889
	0.7789	0.7716	0.7840
2.0	0.4096	0.4015	0.4213
	0.7855	0.7752	0.7886
	0.7797	0.7719	0.7838

Table 6.2.3-4: Variation of expected error

Assmd Obs. err, winds	Assumed Obs. error, heights 5.0	10.0	20.0
0.5	0.4348	0.4287	0.4499
	0.7800	0.7717	0.7856
	0.7748	0.7687	0.7809
1.0	0.4350	0.4287	0.4495
	0.7801	0.7717	0.7855
	0.7749	0.7687	0.7808
2.0	0.4360	0.4287	0.4483
	0.7807	0.7719	0.7853
	0.7754	0.7689	0.7806

Table 6.2.2-3: Variation of expected error

Assmd Obs. err, winds	Assumed Obs. error, heights 5.0	10.0	20.0
0.5	0.3868	0.3771	0.3924
	0.7942	0.7780	0.7879
	0.7864	0.7745	0.7832
1.0	0.3871	0.3771	0.3921
	0.7943	0.7780	0.7877
	0.7866	0.7744	0.7830
2.0	0.3883	0.3774	0.3912
	0.7951	0.7783	0.7875
	0.7873	0.7747	0.7828

Table 6.2.4-3: Variation of expected error

Assmd Obs. err, winds	Assumed Obs. error, heights 5.0	10.0	20.0
0.5	0.4111	0.4025	0.4193
	0.7895	0.7753	0.7848
	0.7824	0.7720	0.7803
1.0	0.4113	0.4025	0. `11
	0.7896	0.7753	C 47
	0.7825	0.7720	0. 02
2.0	0.4123	0.4028	0.4183
	0.7902	0.7755	0.7845
	0.7830	0.7722	0.7800

Table 6.2.3-2: Variation of expected error

Assmd Obs. err, winds	Assumed Obs. error, heights 5.0	10.0	20.0
0.5	0.3854	0.3767	0.3948
	0.7914	0.7778	0.7899
	0.7844	0.7742	0.7851
1.0	0.3857	0.3767	0.3944
	0.7916	0.7778	0.7898
	0.7846	0.7742	0.7849
2.0	0.3870	0.3769	0.3933
	0.7925	0.7780	0.7896
	0.7854	0.7745	0.7847

Table 6.2.4-4: Variation of expected error

Assmd Obs. err, winds	Assumed Obs. error, heights 5.0	10.0	20.0
0.5	0.4091	0.4011	0.4192
	0.7868	0.7747	0.7867
	0.7803	0.7714	0.7820
1.0	0.4093	0.4011	0.4188
	0.7869	0.7747	0.7866
	0.7804	0.7714	0.7818
2.0	0.4104	0.4012	0.4178
	0.7875	0.7749	0.7863
	0.7810	0.7716	0.7816

Table 6.2.3-3: Variation of expected error

Assmd Obs. err, winds	Assumed Obs. error, heights 5.0	10.0	20.0
0.5	0.3872	0.3908	0.4253
	0.7834	0.7872	0.8060
	0.7795	0.7828	0.8003
1.0	0.3869	0.3891	0.4223
	0.7831	0.7864	0.8049
	0.7793	0.7820	0.7993
2.0	0.3872	0.3849	0.4137
	0.7841	0.7852	0.8029
	0.7803	0.7811	0.7975

Table 6.2.4-5: Variation of expected error

Assmd Obs. err, winds	Assumed Obs. error, heights 5.0	10.0	20.0
0.5	0.3106	0.2946	0.3036
	0.7703	0.7240	0.7203
	0.7549	0.7196	0.7167
1.0	0.3112	0.2950	0.3038
	0.7708	0.7243	0.7204
	0.7553	0.7199	0.7168
2.0	0.3136	0.2967	0.3049
	0.7729	0.7258	0.7212
	0.7574	0.7213	0.7176

Table 6.2.5-4: Variation of expected error

Assmd Obs. err, winds	Assumed Obs. error, heights 5.0	10.0	20.0
0.5	0.2952	0.2844	0.3019
	0.7322	0.7119	0.7231
	0.7253	0.7087	0.7192
1.0	0.2961	0.2843	0.3009
	0.7329	0.7118	0.7226
	0.7260	0.7086	0.7188
2.0	0.3001	0.2852	0.2990
	0.7371	0.7132	0.7228
	0.7300	0.7100	0.7190

Table 6.2.5-5: Variation of expected error

Assmd Obs. err, winds	Assumed Obs. error, heights 5.0	10.0	20.0
0.5	0.9359	0.9356	0.9379
	0.9819	0.9817	0.9825
	0.9844	0.9843	0.9847
1.0	0.9359	0.9356	0.9379
	0.9819	0.9817	0.9825
	0.9844	0.9843	0.9847
2.0	0.9359	0.9356	0.9379
	0.9819	0.9817	0.9825
	0.9844	0.9843	0.9847

Table 6.3.1-1: Variation of expected error

Assmd Obs. err, winds	Assumed Obs. error, heights 5.0	10.0	20.0
0.5	0.9916	0.9873	0.9807
	0.9878	0.9879	0.9897
	0.9901	0.9902	0.9908
1.0	0.9907	0.9863	0.9796
	0.9876	0.9878	0.9895
	0.9899	0.9900	0.9907
2.0	0.9872	0.9826	0.9757
	0.9871	0.9872	0.9889
	0.9894	0.9895	0.9901

Table 6.3.1-2: Variation of expected error

Assmd Obs. err, winds	Assumed Obs. error, heights 5.0	10.0	20.0
0.5	0.8889	0.8913	0.9013
	0.9678	0.9669	0.9670
	0.9740	0.9732	0.9723
1.0	0.8890	0.8914	0.9014
	0.9678	0.9669	0.9671
	0.9740	0.9732	0.9724
2.0	0.8892	0.8916	0.9016
	0.9679	0.9670	0.9672
	0.9741	0.9733	0.9724

Table 6.3.2-1: Variation of expected error

Assmd Obs. err, winds	Assumed Obs. error, heights 5.0	10.0	20.0
0.5	0.8581	0.8572	0.8620
	0.9595	0.9587	0.9603
	0.9653	0.9651	0.9658
1.0	0.8581	0.8572	0.8619
	0.9595	0.9587	0.9603
	0.9653	0.9651	0.9658
2.0	0.8583	0.8573	0.8620
	0.9596	0.9587	0.9603
	0.9653	0.9651	0.9658

Table 6.3.2-2: Variation of expected error

Assmd Obs. err, winds	Assumed Obs. error, heights 5.0	10.0	20.0
0.5	0.8680	0.8649	0.8639
	0.9595	0.9590	0.9611
	0.9656	0.9656	0.9667
1.0	0.8680	0.8649	0.8638
	0.9595	0.9590	0.9611
	0.9656	0.9656	0.9667
2.0	0.8681	0.8649	0.8639
	0.9596	0.9590	0.9611
	0.9657	0.9656	0.9668

Table 6.3.2-3: Variation of expected error

Assmd Obs. err, winds	Assumed Obs. error, heights 5.0	10.0	20.0
0.5	0.8284	0.8294	0.8402
	0.9616	0.9604	0.9613
	0.9683	0.9677	0.9675
1.0	0.8284	0.8294	0.8402
	0.9616	0.9604	0.9613
	0.9683	0.9677	0.9675
2.0	0.8286	0.8295	0.8402
	0.9617	0.9604	0.9613
	0.9683	0.9677	0.9676

Table 6.3.3-2: Variation of expected error

Assmd Obs. err, winds	Assumed Obs. error, heights 5.0	10.0	20.0
0.5	0.8212	0.8201	0.8261
	0.9610	0.9600	0.9617
	0.9673	0.9671	0.9677
1.0	0.8212	0.8201	0.8261
	0.9610	0.9600	0.9617
	0.9673	0.9670	0.9677
2.0	0.8213	0.8202	0.8261
	0.9611	0.9601	0.9617
	0.9673	0.9671	0.9678

Table 6.3.3-3: Variation of expected error

Assmd Obs. err, winds	Assumed Obs. error, heights 5.0	10.0	20.0
0.5	0.8047	0.8001	0.7985
	0.9668	0.9667	0.9684
	0.9733	0.9734	0.9743
1.0	0.8030	0.7983	0.7967
	0.9664	0.9662	0.9679
	0.9728	0.9729	0.9739
2.0	0.7984	0.7930	0.7912
	0.9653	0.9647	0.9663
	0.9717	0.9717	0.9727

Table 6.3.4-5: Variation of expected error

Assmd Obs. err, winds	Assumed Obs. error, heights 5.0	10.0	20.0
0.5	0.8266	0.8238	0.8249
	0.9609	0.9602	0.9623
	0.9674	0.9673	0.9683
1.0	0.8266	0.8238	0.8249
	0.9609	0.9602	0.9623
	0.9674	0.9673	0.9683
2.0	0.8268	0.8238	0.8249
	0.9610	0.9602	0.9623
	0.9675	0.9674	0.9684

Table 6.3.3-4: Variation of expected error

Assmd Obs. err, winds	Assumed Obs. error, heights 5.0	10.0	20.0
0.5	0.6957	0.6980	0.7169
	0.9403	0.9370	0.9387
	0.9536	0.9524	0.9522
1.0	0.6960	0.6983	0.7172
	0.9405	0.9372	0.9388
	0.9538	0.9525	0.9523
2.0	0.6972	0.6995	0.7184
	0.9412	0.9379	0.9394
	0.9544	0.9531	0.9529

Table 6.3.5-4: Variation of expected error

Assmd Obs. err, winds	Assumed Obs. error, heights 5.0	10.0	20.0
0.5	0.7810	0.7818	0.7940
	0.9626	0.9612	0.9624
	0.9692	0.9687	0.9689
1.0	0.7810	0.7818	0.7940
	0.9626	0.9612	0.9624
	0.9692	0.9687	0.9689
2.0	0.7812	0.7819	0.7940
	0.9627	0.9613	0.9624
	0.9692	0.9687	0.9689

Table 6.3.4-3: Variation of expected error

Assmd Obs. err, winds	Assumed Obs. error, heights 5.0	10.0	20.0
0.5	0.6842	0.6824	0.6925
	0.9328	0.9307	0.9332
	0.9473	0.9469	0.9479
1.0	0.6843	0.6824	0.6924
	0.9329	0.9306	0.9331
	0.9473	0.9468	0.9478
2.0	0.6852	0.6828	0.6928
	0.9338	0.9310	0.9334
	0.9477	0.9471	0.9481

Table 6.3.5-5: Variation of expected error

Assmd Obs. err, winds	Assumed Obs. error, heights 5.0	10.0	20.0
0.5	0.7787	0.7775	0.7845
	0.9621	0.9610	0.9628
	0.9686	0.9684	0.9691
1.0	0.7787	0.7775	0.7845
	0.9622	0.9610	0.9627
	0.9686	0.9683	0.9691
2.0	0.7789	0.7776	0.7846
	0.9623	0.9611	0.9628
	0.9687	0.9684	0.9691

Table 6.3.4-4: Variation of expected error

APPENDIX 2: SUBROUTINE TCOR

This appendix contains the listing for the subroutine that evaluates the true covariance and cross-covariance function values between a given (grid) point and the observation points.

```
- * - - + - - * - - + - - * - - + - - * - - + - - * - - + - - * - - + -

      SUBROUTINE TCOR(NCF,THD,PHD,NH,TUD,PUD,NU,TVD,PVD,NV,TD,PD,KH,KU,
     1 KV,VAR,CAPPA,CVM,NCVM)
C
C     THIS SUBROUTINE CALCULATES THE TRUE COVARIANCE BETWEEN THE
C     OBSERVATION VARIABLES AND INDICATED VARIABLES AT A GIVEN POINT
C
C     THE ARGUMENTS ARE
C
C     INPUT ARGUMENTS
C     NCF            - COVARIANCE FUNCTION NUMBER
C     THD,PHD;NH     - ARRAY OF HEIGHT OBSERVATION LOCATIONS, NH OF THEM
C     TUD,PUD;NU     - ARRAY OF U-WIND OBSERVATION LOCATIONS, NU OF THEM
C     TVD,PVD;NV     - ARRAY OF V-WIND OBSERVATION LOCATIONS, NV OF THEM
C                      THE ABOVE ARE IN DEGREES, LONGITUDE AND LATITUDE,
C                      RESPECTIVELY
C     KH             - NONZERO IF H COVARIANCE TO BE COMPUTED
C     KU             - NONZERO IF U COVARIANCE TO BE COMPUTED
C     KV             - NONZERO IF V COVARIANCE TO BE COMPUTED
C     VAR            - VARIANCE OF HEIGHT-HEIGHT ERRORS
C     CAPPA          - CORIOLIS CONSTANT
C     TD,PD          - GIVEN (GRID) LOCATION, DEGREES
C     NCVM           - ROW DIMENSION OF CVM ARRAY
C
C     OUTPUT ARGUMENT
C     CVM            - ARRAY OF COVARIANCES BETWEEN OBS VARS AND GRID LOCS
C                      AN NH+NU+NV BY 3 ARRAY
C
      IMPLICIT REAL*8 (A-H,O-Z)
      PARAMETER (NSZ=36)
      DIMENSION THD(NH),PHD(NH),TUD(NU),PUD(NU),TVD(NV),PVD(NV),
     1 CVM(NCVM,3)
      DIMENSION TOH(NSZ),POH(NSZ),TOU(NSZ),POU(NSZ),TOV(NSZ),POV(NSZ)
      DIMENSION AP(5),AAP(5)
      COMMON /IO/KOUT
      DATA NTIME/0/
      DATA AP,AAP/5D-6,3.0825D-6,3.0825D-6,3.0825D-6,2.188D-6,
     1 0D0,0D0,.15D0,.2722D0,.2722D0/
C
C     THIS ROUTINE IS SET UP TO ACCEPT GENERAL (ISOTROPIC) COVARIANCE
C     FUNCTIONS.  THIS REQUIRES THE DEFINITION OF A NUMBER OF ARITHMETIC
C     STATEMENT FUNCTIONS WHICH DEFINE THE DISTANCE FUNCTION IN TERMS OF
C     LATITUDE AND LONGITUDE (PHI AND THETA), ITS DERIVATIVES WRT PHI AN
C     THETA, AS WELL AS THE COVARIANCE FUNCTION AND IT'S DERIVATIVES.
C
C     THE FUNCTIONS NEEDED ARE
C     DIST      - DISTANCE FUNCTION
```

59

```
C      COV     - ISOTROPIC COVARIANCE FUNCTION AS A FUNCTION OF DISTANCE
C      DCOV    - DERIVATIVE OF COV WRT DISTANCE
C      D2COV   - 2ND DERIVATIVE OF COV WRT DISTANCE - DCOV/DISTANCE
C      VARU    - VARIANCE OF U-WIND
C      VARV    - VARIANCE OF V-WIND
C      DSDP    - PARTIAL DIST WRT PHII
C      DSDT    - PARTIAL DIST WRT THETAI
C      DDP1    - PART OF 2ND PARTIAL DIST WRT PHII AND PHIJ
C      DDP2    - PART OF 2ND PARTIAL DIST WRT THETAI AND THETAJ
C      DDP3    - PART OF 2ND PARTIAL DIST WRT PHII AND THETAJ
C
       DATA RAD/6.372D6/
       DIST(P,P1,T,T1)=RAD*DSQRT((P-P1)**2+((T-T1)*COS((P+P1)/2.D0))**2)
       COV(S) = VAR*(OMAA*(1.D0+A*S)*EXP(-A*S)+AA)
       DCOV(S) = -VAR*OMAA*A*A*S*EXP(-A*S)
       D2COV(S) = VAR*OMAA*A**3*S*EXP(-A*S)
       VARU(P) = VAR*OMAA*(RAD*A)**2
       VARV(P) = VAR*OMAA*(RAD*A*COS(P))**2
       DSDP(P,P1,T,T1,S) = RAD**2/S*(-(T-T1)**2*SIN(P+P1)/4.D0+(P-P1))
       DSDT(P,P1,T,T1,S) = RAD**2/S*(T-T1)*COS((P+P1)/2.D0)**2
       DDP1(P,P1,T,T1,S) = RAD**2/S*(1.D0 + (T-T1)**2*COS(P+P1)/4.D0)
       DDP2(P,P1,T,T1,S) = (RAD*COS((P+P1)/2.D0))**2/S
       DDP3(P,P1,T,T1,S) = RAD**2/S*(T-T1)*SIN(P+P1)/2.D0
       IF(NTIME.NE.NCF) THEN
C      SET PARAMETERS FOR THIS FUNCTION NUMBER
C
         NCFR=MAX(1,NCF)
         NCFR=MIN(NCFR,5)
         A = AP(NCFR)
         AA = AAP(NCFR)
         OMAA = 1.D0-AA
         WRITE(KOUT,1)A,AA
         PI=DATAN(1.D0)*4.D0
         DTR = PI/180.D0
         NTIME = NCF
       ENDIF
C
C      CONVERT LOCATIONS TO RADIANS
C
       DO 100 I=1,NH
         POH(I) = PHD(I)*DTR
         TOH(I) = THD(I)*DTR
 100   CONTINUE
       DO 110 I=1,NU
         POU(I) = PUD(I)*DTR
         TOU(I) = TUD(I)*DTR
 110   CONTINUE
       DO 120 I=1,NV
         POV(I) = PVD(I)*DTR
         TOV(I) = TVD(I)*DTR
 120   CONTINUE
       P = PD*DTR
       T = TD*DTR
C
```

```
C       START CALCULATIONS
        K = 0
        SP = SIN(P)
        CP = COS(P)
        IF(NH.NE.0) THEN
            DO 200 I=1,NH
                K = K + 1
                S = DIST(P,POH(I),T,TOH(I))
                DF = DCOV(S)
                IF(KH.GT.0) CVM(K,1) = COV(S)
                CVM(K,2) = 0.D0
                CVM(K,3) = 0.D0
                IF(KU.GT.0 .AND. S.GT.0.D0)
     1            CVM(K,2) = DF*DSDP(P,POH(I),T,TOH(I),S)
                IF(KV.GT.0 .AND. S.GT.0.D0)
     1            CVM(K,3) = DF*DSDT(P,POH(I),T,TOH(I),S)
                CVM(K,2) = -CVM(K,2)*CAPPA/SP
                CVM(K,3) = CVM(K,3)*CAPPA/CP/SP
200         CONTINUE
        ENDIF
        IF(NU.NE.0) THEN
            DO 220 I=1,NU
                K = K + 1
                S = DIST(P,POU(I),T,TOU(I))
                DF = DCOV(S)
                DD2 = D2COV(S)
                SPI = SIN(POU(I))
                CPI = COS(POU(I))
                CVM(K,1) = 0.D0
                IF(KH.GT.0 .AND. S.GT.0.D0)
     1            CVM(K,1) = DF*DSDP(POU(I),P,TOU(I),T,S)
                CVM(K,2) = VARU(P)
                IF(KU.GT.0 .AND. S.GT.0.D0)
     1            CVM(K,2) = -DF*DDP1(POU(I),P,TOU(I),T,S) +
     2             DD2*DSDP(P,POU(I),T,TOU(I),S)*DSDP(POU(I),P,TOU(I),T,S)
                CVM(K,3) = 0.D0
                IF(KV.GT.0 .AND. S.GT.0.D0)
     1          CVM(K,3) = -DF*DDP3(P,POU(I),T,TOU(I),S) +
     2            DD2*DSDP(POU(I),P,TOU(I),T,S)*DSDT(P,POU(I),T,TOU(I),S)
                CVM(K,1) = -CVM(K,1)*CAPPA/SPI
                CVM(K,2) = CVM(K,2)*CAPPA**2/SP/SPI
                CVM(K,3) = -CVM(K,3)*CAPPA**2/SP/CP/SPI
220         CONTINUE
        ENDIF
        IF(NV.GT.0) THEN
            DO 240 I=1,NV
                K = K + 1
                S = DIST(P,POV(I),T,TOV(I))
                DF = DCOV(S)
                DD2 = D2COV(S)
                SPI = SIN(POV(I))
                CPI = COS(POV(I))
                CVM(K,1) = 0.D0
                IF(KH.GT.0 .AND. S.GT.0.D0)
```

```
   1         CVM(K,1) = DF*DSDT(POV(I),P,TOV(I),T,S)
           CVM(K,2) = 0.D0
           IF(KU.GT.0 .AND. S.GT.0.D0)
   1          CVM(K,2) = -DF*DDP3(POV(I),P,TOV(I),T,S) +
   2           DD2*DSDP(P,POV(I),T,TOV(I),S)*DSDT(POV(I),P,TOV(I),T,S)
           CVM(K,3) = VARV(P)
           IF(KV.GT.0 .AND. S.GT.0.D0)
   1          CVM(K,3) = -DF*DDP2(P,POV(I),T,TOV(I),S) +
   2           DD2*DSDT(POV(I),P,TOV(I),T,S)*DSDT(P,POV(I),T,TOV(I),S)
           CVM(K,1) = CVM(K,1)*CAPPA/CPI/SPI
           CVM(K,2) = -CVM(K,2)*CAPPA**2/CPI/SPI/SP
           CVM(K,3) = CVM(K,3)*CAPPA**2/CPI/CP/SP/SPI
 240     CONTINUE
    ENDIF
    RETURN
  1 FORMAT(' TCOR - 01/12/90:   2ND AR, A,AA = ',1P,2E11.3)
    END
```

INITIAL DISTRIBUTION LIST

ASST. FOR ENV. SCIENCES
ASST. SEC. OF THE NAVY (R&D)
ROOM 5E731, THE PENTAGON
WASHINGTON, DC   20350

OFFICE OF NAVAL RESEARCH
CODE 422AT
ARLINGTON, VA   22217

COMMANDING OFFICER
FLENUMOCEANCEN
MONTEREY, CA   93943

NAVAL POSTGRADUATE SCHOOL
METEOROLOGY DEPT.
MONTEREY, CA   93943

LIBRARY (2)
NAVAL POSTGRADUATE SCHOOL
MONTEREY, CA   93943

COMMANDER
NAVAIRSYSCOM (AIR-330)
WASHINGTON, DC   20361

USAFETAC/TS
SCOTT AFB, IL   62225

AFGWC/DAPL
OFFUTT AFB, NE   68113

AFGL/OPI
HANSCOM AFB, MA   01731

COMMANDER & DIRECTOR
ATTN: DELAS-D
U.S. ARMY ATMOS. SCI. LAB
WHITE SAND MISSILE RANGE
WHITE SANDS, NM   88002

NOAA-NESDIS LIAISON
ATTN: CODE SC2
NASA-JOHNSON SPACE CENTER
HOUSTON, TX   77058

ACQUISITIONS SECT. IRDB-DB23
LIBRARY & INFO. SERV., NOAA
6009 EXECUTIVE BLVD.
ROCKVILLE, MD   20852

NATIONAL WEATHER SERVICE
WORLD WEATHER BLDG., RM 307
5200 AUTH ROAD
CAMP SPRINGS, MD   20023

DIRECTOR
GEOPHYS. FLUID DYNAMICS LAB
NOAA, PRINCETON UNIVERSITY
P.O. BOX 308
PRINCETON, NJ   08540

LABORATORY FOR ATMOS. SCI.
NASA GODDARD SPACE FLIGHT CEN.
GREENBELT, MD   20771

COLORADO STATE UNIVERSITY
ATMOSPHERIC SCIENCES DEPT.
ATTN; DR. WILLIAM GRAY
FORT COLLINS, CO   80523

CHAIRMAN, METEOROLOGY DEPT.
UNIVERSITY OF OKLAHOMA
NORMAN, OK   73069

COLORADO STATE UNIVERSITY
ATMOSPHERIC SCIENCES DEPT.
ATTN; LIBRARIAN
FT. COLLINS, CO   80523

UNIVERSITY OF WASHINGTON
ATMOSPHERIC SCIENCES DEPT.
SEATTLE, WA   98195

FLORIDA STATE UNIVERSITY
ENVIRONMENTAL SCIENCES DEPT.
TALLAHASSEE, FL   32306

DIRECTOR
COASTAL STUDIES INSTITUTE
LOUISIANA STATE UNIVERSITY
ATTN: O. HUH
BATON ROUGE, LA   70803

UNIVERSITY OF MARYLAND
METEOROLOGY DEPT.
COLLEGE PARK, MD   20742

CHAIRMAN
METEOROLOGY DEPT.
MASSACHUSETTS INSTITUTE OF
  TECHNOLOGY
CAMBRIDGE, MA   02139

ATMOSPHERIC SCIENCES CENTER
DESERT RESEARCH INSTITUTE
P.O. BOX 60220
RENO, NV 89506

CENTER FOR ENV. & MAN, INC.
RESEARCH LIBRARY
275 WINDSOR ST.
HARTFORD, CT 06120

METEOROLOGY RESEARCH, INC.
464 W. WOODBURY RD.
ALTADENA, CA 91001

CONTROL DATA CORP.
METEOROLOGY DEPT. RSCH. DIV.
2800 E. OLD SHAKOPEE RD.
BOX 1249
MINNEAPOLIS, MN 55440

OCEAN DATA SYSTEMS, INC.
2460 GARDEN ROAD
MONTEREY, CA 93940

DIRECTOR OF RESEARCH   (2)
 ADMINISTRATION
CODE 012
NAVAL POSTGRADUATE SCHOOL
MONTEREY, CA 93943

PROFESSOR H. FREDRICKSEN
CHAIRMAN, DEPT OF MATHEMATICS
NAVAL POSTGRADUATE SCHOOL
MONTEREY, CA 93943

DR. RICHARD LAU
OFFICE OF NAVAL RESEARCH
800 QUINCY ST.
ARLINGTON, VA 22217

PROFESSOR G.M. NIELSON
DEPT. OF COMPUTER SCIENCE
ARIZONA STATE UNIVERSITY
TEMPE, AZ 85287

DR. H. JEAN THIEBAUX
NATIONAL METEOROLOGICAL CENTER
DEVELOPMENT DIVISION
WASHINGTON, DC 20233

PROFESSOR PETER ALFELD
DEPARTMENT OF MATHEMATICS
UNIVERSITY OF UTAH
SALT LAKE CITY, UT 84112

MR. ROSS HOFFMAN
ATMOSPHERIC AND ENVIRONMENTAL
 RESEARCH, INC.
840 MEMORIAL DRIVE
CAMBRIDGE, MA 02139

DR. WILLIAM A. HOPPEL
OFFICE OF NAVAL RESEARCH
800 QUINCY ST.
ARLINGTON, VA 22217

DR. DAVID F. PARRISH
NATIONAL METEOROLOGICAL CENTER
NWS
NOAA
WASHINGTON, DC 20233

CHIEF OF NAVAL RESEARCH (2)
LIBRARY SERVICES, CODE 784
BALLSTON TOWER #1
800 QUINCY ST.
ARLINGTON, VA 22217

COMMANDING OFFICER
NOARL
NSTL, MS 39529

SUPERINTENDENT
LIBRARY REPORTS
U. S. NAVAL ACADEMY
ANNAPOLIS, MD 21402

NAVAL POSTGRADUATE SCHOOL
OCEANOGRAPHY DEPT.
MONTEREY, CA 93943

COMMANDER   (2)
NAVAIRSYSCOM
ATTN: LIBRARY (AIR-7226)
WASHINGTON, DC 20361

COMMANDER
NAVOCEANSYSCEN
DR. J. RICHTER, CODE 532
SAN DIEGO, CA 92152

DR. JOHN HOVERMALE
DIRECTOR, ATMOSPHERIC SCIENCES
 DIVISION
NAVAL OCEANOGRAPHIC AND
 ATMOSPHERIC RESEARCH LABORATORY
MONTEREY, CA 93943

SUPERINTENDENT
ATTN: USAFA (DEG)
COLORADO SPRINGS, CO 80840
AFGL/LY
HANSCOM AFB, MA 01731

OFFICER IN CHARGE
SERVICE SCHOOL COMMAND
DET. CHANUTE/STOP 62
CHANUTE AFB, IL 61868

DIRECTOR   (2)
DEFENSE TECH. INFORMATION
 CENTER, CAMERON STATION
ALEXANDRIA, VA 22314

DIRECTOR
NATIONAL METEOROLOGICAL CENTER
NWS, NOAA
WWB W32, RM 204
WASHINGTON, DC 20233

DIRECTOR
OFFICER OF PROGRAMS RX3
NOAA RESEARCH LAB
BOULDER, CO 80302

DIRECTOR
NATIONAL SEVERE STORMS LAB
1313 HALLEY CIRCLE
NORMAN, OK 73069

DIRECTOR
TECHNIQUES DEVELOPMENT LAB
GRAMAX BLDG.
8060 13TH ST.
SILVER SPRING, MD 20910

EXECUTIVE SECRETARY, CAO
SUBCOMMITTEE ON ATMOS. SCI.
NATIONAL SCIENCE FOUNDATION
RM. 510, 1800 G. STREET, NW
WASHINGTON, DC 20550

ATMOSPHERIC SCIENCES DEPT.
UCLA
405 HILGARD AVE.
LOS ANGELES, CA 90024

CHAIRMAN, METEOROLOGY DEPT.
CALIFORNIA STATE UNIVERSITY
SAN JOSE, CA 95192

NATIONAL CENTER FOR ATMOS.
 RSCH., LIBRARY ACQUISITIONS
P.O. BOX 3000
BOULDER, CO 80302

CHAIRMAN, METEOROLOGY DEPT.
PENNSYLVANIA STATE UNIVERSITY
503 DEIKE BLDG.
UNIVERSITY PARK, PA 16802

UNIVERSITY OF HAWAII
METEOROLOGY DEPT.
2525 CORREA ROAD
HONOLULU, HI 96822

ATMOSPHERIC SCIENCES DEPT.
OREGON STATE UNIVERSITY
CORVALLIS, OR 97331

CHAIRMAN
ATMOS. SCIENCES DEPT.
UNIVERSITY OF VIRGINIA
CHARLOTTESVILLE, VA 22903

CHAIRMAN, METEOROLOGY DEPT.
UNIVERSITY OF UTAH
SALT LAKE CITY, UT 84112

ATMOSPHERIC SCI. RSCH. CENTER
NEW YORK STATE UNIVERSITY
1400 WASHINGTON AVE.
ALBANY, NY 12222

METEOROLOGY INTL., INC.
P.O. BOX 22920
CARMEL, CA 93922

SCIENCE APPLICATIONS, INC.
205 MONTECITO AVENUE
MONTEREY, CA 93940

EUROPEAN CENTRE FOR MEDIUM
 RANGE WEATHER FORECASTS
SHINFIELD PARK, READING
BERKSHIRE RG2 9AX, ENGLAND

DEPT. OF MATHEMATICS
NAVAL POSTGRADUATE SCHOOL
MONTEREY, CA 93943

PROFESSOR R. FRANKE, MA/FE
DEPT. OF MATHEMATICS   (10)
NAVAL POSTGRADUATE SCHOOL
MONTEREY, CA 93943

PROFESSOR R.E. BARNHILL
DEPT. OF COMPUTER SCIENCE
ARIZONA STATE UNIVERSITY
TEMPE, AZ   85287

LIBRARY, FLEET NUMERICAL   (2)
 OCEANOGRAPHY CENTER
MONTEREY, CA   93943

PROFESSOR GRACE WAHBA
DEPARTMENT OF STATISTICS
UNIVERSITY OF WISCONSIN
MADISON, WI   53705

DR. R.S. SEAMAN
AUSTRALIAN NUMERICAL
 METEOROLOGY RESEARCH CENTRE
P.O. BOX 5089AA
MELBOURNE, VICTORIA,
AUSTRALIA, 3001

PROFESSOR MARK E. HAWLEY
DEPARTMENT OF ENVIRONMENTAL
  SCIENCES
UNIVERSITY OF VIRGINIA
CHARLOTTESVILLE, VA   22903

PROFESSOR JAMES J. O'BRIEN
DEPARTMENT OF METEOROLOGY
THE FLORIDA STATE UNIVERSITY
TALLAHASSEE, FLORIDA   32306

NAVAL OCEANOGRAPHIC AND   (6)
 ATMOSPHERIC RESEARCH LABORATORY
ATTN: DR. EDWARD BARKER
        DR. THOMAS ROSMOND
        DR. JAMES GOERSS
        NANCY BAKER
        PAT PHOEBUS
        LARRY PHEGLEY
MONTEREY, CA   93943

DR. LICIA LENARDUZZI
CNR-IAMI
VIA A. M. AMPERE, 56
20131 MILANO
ITALIA

DR. LAWRENCE C. BREAKER
NATIONAL METEOROLOGICAL CENTER
MARINE PREDICTION BRANCH
WASHINGTON, DC   20233

DR. LEV GANDIN
NATIONAL METEOROLOGICAL CENTER
DEVELOPMENT DIVISION
WASHINGTON, DC   20233

DR. ANDREW LORENC
BRITISH MET. OFFICE
BRACKNELL RB12 2SZ
BERKS., ENGLAND

DEAN G. DUFFY
NASA/GODDARD SPACE FLIGHT CENTER
LABORATORY FOR ATMOSPHERES
GREENBELT, MD   20771

DR. EMMETT MADDRY
K-43
NAVAL SURFACE WARFARE CENTER
DAHLGREN, VA 22448-5000

COMMANDING OFFICER   (2)
NAVAL OCEANOGRAPHIC AND
 ATMOSPHERIC RESEARCH LABORATORY
ATTN: DR. MOSELY
NSTL, MS 39529